VILNIUS UNIVERSITY

ARUNAS MIASOJEDOVAS

CONTROL OF FLUORESCENCE PROPERTIES OF ORGANIC OPTOELECTRONIC MATERIALS BY MOLECULAR AGGREGATE FORMATION

Summary of doctoral dissertation
Physical sciences, Physics (02 P)

Vilnius, 2013

The research has been carried out in 2009–2013 at the Semiconductor Physics Department of Physics Faculty and Institute of Applied Research, Vilnius University.

Scientific supervisor:

Prof. habil. dr. Saulius Antanas Juršėnas (Vilnius University, Physical Sciences, Physics – 02 P).

Council of defense of the doctoral thesis of Physical Sciences at Vilnius University:

Chairman:

Prof. habil. dr. Gintautas Tamulaitis (Vilnius University, Physical Sciences, Physics – 02 P).

Members:

Dr. Šarūnas Meškinis (Kaunas University of Technology, Physical Sciences, Physics – 02 P).

Prof. habil. dr. Sigitas Tamulevičius (Kaunas University of Technology, Physical Sciences, Physics – 02 P).

Prof. habil. dr. Sigitas Tumkevičius (Vilnius University, Physical Sciences, Chemistry – 03 P)

Prof. habil. dr. Gintaras Valušis (Vilnius University, Physical Sciences, Physics – 02 P).

Opponents:

Dr. Kristijonas Genevičius (Vilnius University, Physical Sciences, Physics – 02 P).

Dr. Tadas Malinauskas (Kaunas University of Technology, Physical Sciences, Chemistry – 03 P).

The official defense of the doctoral thesis will be held in the public session of the Vilnius university Defense Council of Physical sciences at 15 h on September 27, 2013, in 212 lecture room of Faculty of Physics, Vilnius University, Saulėtekio Ave. 9-III, LT-10222 Vilnius, Lithuania.

The summary of the doctoral thesis has been distributed on August …. , 2013.

The doctoral thesis is available at Vilnius University library and at the library of Center for Physical Sciences and Technology.

VILNIAUS UNIVERSITETAS

ARŪNAS MIASOJEDOVAS

ORGANINĖS OPTOELEKTRONIKOS MEDŽIAGŲ FLUORESCENCIJOS SAVYBIŲ VALDYMAS FORMUOJANT MOLEKULINIUS AGREGATUS

Daktaro disertacijos santrauka

Fiziniai mokslai, fizika (02 P)

Vilnius, 2013

Disertacija rengta Vilniaus universiteto Fizikos fakulteto Puslaidininkių fizikos katedroje ir Taikomųjų mokslų institute 2009 – 2013 metais.

Mokslinis vadovas:

Prof. habil. dr. Saulius Antanas Juršėnas (Vilniaus universitetas, fiziniai mokslai, fizika – 02 P)

Disertacija ginama Vilniaus Universiteto Fizikos mokslų krypties taryboje:

Pirmininkas:

Prof. habil. dr. Gintautas Tamulaitis (Vilniaus Universitetas, fiziniai mokslai, fizika – 02 P).

Nariai:

Dr. Šarūnas Meškinis (Kauno technologijos universitetas, fiziniai mokslai, fizika – 02 P).

Prof. habil. dr. Sigitas Tamulevičius (Kauno technologijos universitetas, fiziniai mokslai, fizika – 02 P).

Prof. habil. dr. Sigitas Tumkevičius (Vilniaus Universitetas, fiziniai mokslai, chemija – 03 P)

Prof. habil. dr. Gintaras Valušis (Vilniaus Universitetas, fiziniai mokslai, fizika – 02 P).

Oponentai:

Dr. Kristijonas Genevičius (Vilniaus Universitetas, fiziniai mokslai, fizika – 02 P).

Dr. Tadas Malinauskas (Kauno technologijos universitetas, fiziniai mokslai, chemija – 03 P).

Disertacija bus ginama viešame Fizikos mokslų krypties tarybos posėdyje 2013 m. rugsėjo 27 dieną 15 valandą Vilniaus universiteto Fizikos fakulteto 212 auditorijoje, Saulėtekio al. 9, III rūmai, LT-10222 Vilnius, Lietuva.

Disertacijos santrauka išsiuntinėta 2013 m. rugpjūčio .... d.

Disertaciją galima peržiūrėti Vilniaus univesiteto ir Fizinių ir technologijos mokslų centro bibliotekose.

Santrauka

Organinė elektronika pastaruoju metu yra viena sparčiausiai besiplėtojančių puslaidininkių prietaisų krypčių. Ši kryptis labai sparčiai vystoma dėl nuolat kuriamų naujų organinių junginių ir tobulėjančių inžinerijos galimybių. Modernios organinės elektronikos medžiagos yra daugiafunkcinės – tai leidžia ne tik pagerinti medžiagos savybes, bet ir supaprastinti prietaisų gamybos technologiją. Šiame darbe didžiausias dėmesys skiriamas daugiafunkcinių organinių spinduolių fotofizikinių savybių valdymui.

Pagrindinis šios disertacijos tikslas – ištirti daugiafunkcinių molekulinių spinduolių agregacijos nulemtus reiškinius ir jų valdymo galimybes optimizuojant sluoksnio funkcines savybes tokias kaip plėvėdaros savybės, krūvio pernaša, emisijos našumas, spalvinės savybės, sustiprintos savaiminės spinduliuotės slenkstis ir kt. Molekulių struktūra-funkcija savybių supratimas ir spinduolių tolesnio optimizavimo rekomendacijų formulavimas yra vienas svarbiausių šio darbo uždavinių.

Disertacija yra sudaryta iš trijų skyrių, suskirstytų į smulkesnius poskyrius. Pirmasis skyrius yra skirtas įvadui, kuriame pateikti darbo tikslai ir uždaviniai, darbo naujumas ir ginamieji teiginiai. Disertacijos pradžioje yra disertanto kartu su bendraautoriais publikuotų mokslinių straipsnių (tiek įtrauktų, tiek neįtrauktų į disertaciją), taip pat pranešimų konferencijose, kuriose pristatyti disertacijoje pateikti moksliniai tyrimai, sąrašas.

Antrajame disertacijos skyriuje trumpai aprašomi tyrimų metodai ir bandinių paruošimo technologijos.

Trečiasis skyrius yra sudarytas iš dviejų dalių. Pirmoje dalyje supažindinama su agregacijos iššauktu fluorescencijos išaugimo reiškiniu ir jo taikymu fluoresceciniams jutikliams. Pradžioje apžvelgiama literatūra fluorescuojančių organinių nanoagregatų (FON) tema, toliau pateikiami spektroskopiniai fenilendiacetonitrilo junginių FON tyrimo rezultatai ir šių darinių galimas panaudojimas organinių tirpiklių garų fluoresceciniam jutikliui. Šio skyriaus rezultatai detaliai aprašyti [S1, S2, S7] darbuose. Antrasis poskyris skirtas polinių naftalenimido ir trifenilamino junginių optiniam charakterizavimui ir šių junginių galimam temperatūros-laiko fluorescecinio jutiklio taikymui. Šio skyriaus rezultatai yra publikuoti [S8, S10, S11] darbuose.

Antroji trečio skyriaus dalis aprašo molekulių agregacijos nulemto fluorescencijos gesinimo valdymo problemas lazerinėse sistemose. Ši dalis yra suskirstyta į keturis skirsnius. Pirmame skirsnyje pateikiama organinių lazerinių sistemų ir jų medžiagų apžvalga. Antrame skirsnyje pateikiami perileno diimido junginių su pakaitais įlankos vietoje optinių savybių tyrimai ir sustiprintos savaiminės spinduliuotės slenksčio įvertinimas. Šio skyriaus rezultatai yra publikuoti [S3] darbe. Toliau pateikiami DCM tipo dažalų lazeriniams taikymams spektroskopiniai tyrimai. Šio skirsnio rezultatai yra publikuoti [S5, S6] darbuose. Paskutinis skirsnis skirtas fluoreno, karbazolo ir pireno darinių optiniam charakterizavimui ir sustiprintos savaiminės spinduliuotės slenksčio įvertinimui. Šio skirsnio rezultatai detaliai aprašyti [S4] darbe.

Kiekvieno skyriaus pabaigoje yra pateikiami pagrindiniai rezultatai ir išvados. Taip pat yra pateikiamos rekomendacijos tolesniam junginių tobulinimui ir medžiagų pritaikymui. Bendras visuose skyriuose cituotos literatūros sąrašas yra pateikiamas darbo pabaigoje.

Introduction

Currently, organic electronics is one of the most expanding technology of semiconductor devices. This direction is rapidly developing due to the constant synthesis of new organic compounds and sophisticated advances in device engineering. Currently, organic materials are used in organic light-emitting diodes (OLEDs), organic thin-film transistors, solar cells and sensors. Low-cost manufacturing techniques such as wet casting or inkjet printing enable organic materials use in large-area and flexible electronic devices.

Until now, organic optoelectronic devices were based on multi-layer structures and rather simple molecules, where each layer of device was performing its own function - such as the charge carrier injection, transport, emission and others. The optimization of device was performed by optimization of multilayer structure itself. Modern organic electronic materials are multifunctional – this enables not only to improve the material properties, but also to simplify the device architecture. However, the complexity of the molecular structure rises up new problems associated with complex phenomena of the new multifunctional molecules -such as the formation of aggregates, intramolecular charge transfer, intramolecular torsion and others. Therefore, the control of the features of new multifunctional molecules is the main task of organic electronics technology.

This work focuses on the control of photophysical characteristics of multifunctional organic emitters. Since molecules in organic electronic devices are used in the solid state, control of the aggregation related phenomena is one of the biggest problems. Aggregation usually results in decrease of luminescence efficiency due to enhanced exciton migration. Therefore, the most important task in development of efficient organic emitters is reduction of fluorescence concentration quenching. Recently the opposite phenomenon was discovered in certain materials, when in the solution luminescence quantum yield is low, and in the aggregate state emission efficiency increases significantly. Aggregation-induced emission (AIE) effect enables to use these materials in organic luminophore technology and to develop various fluorescent sensors. In this work, we examine the fluorescence characteristics of new multifunctional emitters upon their aggregation and analyse the impact of functional groups on optical properties of the films.

Work goals and objectives

Exploitation of complex molecular systems sets new tasks for chemical synthesis as well as for understanding of their physical properties. Increased number of degrees of freedom makes control of molecular system properties much more complex. Possibility of different molecular conformations, structural disorder, intramolecular charge transfer, variation in the strength of electronic and vibronic system coupling and complexity of the system itself make this control hardly predictable. Having in mind infinite diversity of organic structures, common criteria for selection of particular molecular systems are not formulated yet. In practice, research of some particular molecular systems reveals tendencies towards controlling possibilities only for those particular molecule classes. Therefore understanding of excitation dynamics in complex molecular systems and control of the multifunctional system properties is a hot topic in organic electronics and, more generally, of nanoscience.

In this work, we study aggregation induced emission and quenching of multifunctional molecular emitters and the possibilities to control these phenomena by optimizing functional properties of the solid layers such as film forming properties, charge transfer, the emission efficiency, color features, amplified spontaneous emission threshold and others.

All molecular systems investigated in this work are new. Understanding of structure-property-function relations of the molecules and formulation of recommendations for further optimization of emitters is one of the most important goals of this work.

Dealing with aggregation related phenomena the research objectives are dual. On the one hand, we will investigate optical properties of multifunctional molecules, particularly focusing on the aggregation induced fluorescence changes, such as fluorescence enhancement or pronounced color changes, which we will apply for formation of sensor systems. On the other hand we will try to avoid a negative impact of aggregation quenching by optimizing multifunctional laser emitters aiming to form more effective emissive layer.

Main objectives:

• To investigate optical properties and fluorescence enhancement by forming the molecular aggregates in aqueous solution of new multifragment phenylenediacetonitrile compounds and to form fluorescent ON-OFF sensors; and to investigate optical characteristics of polar naphthalenimide and triphenyamine derivatives in different environments and by forming molecular aggregates and to utilise these compounds for the fluorescent temperature-time sensing layers.

• To investigate the aggregation characteristics and fluorescence concentration quenching by optimizing the amplified spontaneous emission properties of multifunctional lasing systems based on perylene diimide, pyrene and DCM core.

Novelty

In this work, we study new multifragment multifunction emitters and for the first time describe their photophysical properties. The main new results are as follows:

• phenylenediacetonitrile derivatives shows AIE effect due to the steric hindrance of nitrile groups, this effect is controlled by a different size and polarity of the end groups of the molecule;

• singly-bonded triphenylamine and naphthalenimide derivatives show pronounced solvatochromic effect both in solutions (up to 205 nm) and in the solid state in nonpolar surrounding by increase of the dye concentration (up to 91 nm);

• electron-withdrawing bay substituents of the new perylene diimide compounds enable tuning the color of the emission (from 550 to 660 nm) with reasonable fluorescence quantum yield of 50%. At the same time these substituents allowed to increase the concentration of molecules in the polymer matrix, thereby reducing the fluorescence concentration quenching and keeping low the amplified spontaneous emission thresholds; optimal concentration of molecules for lasing layer formation was identified to be 0.5-3 wt %;

• impact of intramolecular twisting on emission properties of singly-bonded pyrene-carbazole/fluorene dyads and triads was revealed for the first time.

Statements to defend:

1. Fluorescent organic nanoparticles formed by re-precipitation method from sterically hindered phenylenediacetonitrile derivatives are suitable for fluorescent organic vapor sensors with fluorescence ON-OFF switching ratio of 38. The nanoparticle size

tuning (from 55 to 360 nm) was achieved by controlling tetrahydrofuran/water mixture ratio with the water concentration in the solution varied from 60 to 90%.

2. Triphenylamine and naphthalimide derivatives show high fluorescence quantum yield up to 70% in solution and up to 60% in polystyrene matrix and due to dipolar character demonstrate pronounced solvatochromic changes in solutions from 548 nm in non-polar solvent to 754 nm in polar solvent and in solid state by changing molecule concentration in non-polar medium (polystyrene) from 542 nm at 0.06% wt to 633 nm at 10% wt. The time-temperature fluorescent sensing layers based on the temperature induced reverse color change, from emission at 610 nm typical for aggregate state to 570 nm typical for single molecule, was demonstrated by thermal treatment at 200^{o}C for 24h.
3. Bulk substituents at bay position of perylene diimide compounds allow changing the fluorescence color (from 550 to 660 nm), significantly reduce the excitonic coupling and thus fluorescence concentration quenching. Bromo-substituted and 2,4-di (trifluoromethyl) phenyl-substituted perylene diimide compounds dispersed in polystyrene matrix form amorphous states, which allows to reach amplified spontaneous emission threshold of 70-200 kW/cm^2 at doping concentration of 0.25 to 2 wt % with high photostability better than in similar systems (with bay substituted phenoxi groups).
4. Intramolecular twisting of singly-bonded pyrene and fluorene/carbazole di-substituted derivatives allows to increase the fluorescence quantum yield up to η = 0.82, and reduce the fluorescence lifetime up to 1 ns, compared to monosubstituted compounds. This leads to a low (20 kW/cm^2) amplified spontaneous emission threshold at high doping concentrations (up to 5 wt %). The sterically hindered dihexyl groups allowed significant reduction of the concentration quenching and achievement of a high emission efficiency (η up to 0.63) in the unencapsulated neat films.

Layout of the thesis

The thesis consists of three chapters and reference list (143 titles). The text is written in Lithuanian language on 116 pages with illustrations presented in 52 figures and 10 tables.

An introduction, main goals and statements to defend as well as the articles and conference contributions of the author together with co-authors are listed at the **first chapter** of the thesis.

The experimental techniques, sample preparation and measurement instrumentation are briefly described in **chapter 2**. In this work, we investigated the molecular systems in different environments: dilute solutions, when molecules were diluted in spectroscopic grade solvents with different polarity, and solid state when molecules were embedded in rigid polymer matrix to reveal possible conformational changes upon photoexcitation, as well as in the neat films to study the excitonic effects. Also fluorescent organic nanoparticles (FON) were formed by re-precipitation method.

All original results are presented in **chapter 3**. They represent extended study of optical properties of new multifunctional fluorescent emitters with special emphasis on aggregation related phenomena. In the first part, we describe the fluorescence changes induced by aggregation and demonstrate the applicability of the materials for fluorescence sensing systems. In the second part, we analyse the aggregation caused quenching (ACQ) and optimise emitting layers suitable for lasing systems.

3. Control of fluorescence properties by aggregate formation

3.1. Aggregation induced emission and color changes

3.1.1. Formation of fluorescent organic nanoparticles and their applications

Low dimensionality accompanied with the fascinating optical, electronic, chemical and mechanical properties, different from those of isolated molecules or bulk material, enabled organic nanoparticles to penetrate the application areas of photovoltaics [1], light-emitting devices [2,3], field-effect transistors [4], biological and fluorescent labels [5], photocatalysis [6], bio- and chemo-sensors [7–9]. While still in the premature stage, the research area covering organic nanoparticles technology mainly focuses on the structure-properties relationships of the aggregate nanostructures and their constituent molecules in attempt to build high-performance nanodimensional structures for organic optoelectronic applications [10]. Among the variety of nanoparticle fabrication methods such as mechanical milling [11] or laser ablation [12] of microcrystalline powders, vapor-driven self-assembly of molecules in polymer matrix [13] and others, the aqueous-solution-based methods like emulsion [1,14] and repricipitation [14,15] are the most popular and frequently used. The advantages of the repricipitation approach lie in the simplicity of nanoparticle preparation, purity of obtained nanoparticle suspensions carrying no surfactants/additives (these are persistently used in miniemulsion process), aqueous processability and easy tunability of the nanoparticle size by adjusting solute concentration, solvent/nonsolvent ratio, temperature etc.

Fluorescent organic nanoparticles (FONs) distinguished by high fluorescence efficiency are particularly attractive for organic light-emitting diodes, labeling and sensing applications due to their high brightness and long-term stability [15,16]. Formation of the FONs involves a certain type of molecules exhibiting unusual fluorescence turn-on in the aggregated form, so called aggregation-induced emission (AIE) phenomenon. The fluorescence turn-on in the solid phase is very uncommon, since usually, intermolecular interactions enhance nonradiative deactivation resulting in emission quenching. AIE is known to be driven by the specific molecular packing along

with the restricted intramolecular rotational/vibrational motions [15,17,18]. The emission enhancement of several orders in magnitude is possible [15]. Although the processes of intramolecular conformational changes and charge-tranfer reaction leading to significant alteration of emission color and intensity were already known [19]. It is claimed that AIE feature was first unveiled in siloles [20] possessing rotating peripheral aromatic rings and later on also observed in 1-cyano-trans- 1,2- bis (4- methylbiphenyl) ethylene [15], diphenyldistyryl- benzenes [21], fumaronitriles [22], triarylethenes [23], azobenzenes [24], diphenyl- dibenzofulvenes [17] and some other compounds. Typically, these molecules are completely non-fluorescent in a solution because of the intramolecular torsions effectively contributing to the non-radiative relaxation pathway. However, aggregation-induced blockage of the molecular conformations occurring on a femtosecond-time-scale closes the non-radiative deactivation channel, and thus, strongly enhances emission in the aggregates [21]. If targeting aggregates with AIE property, special attention must be paid to the molecular structure, which apart from the torsional motions is also responsible for the molecule arrangement in the aggregates, and therefore determines strength and character of intermolecular interactions. More planar and rigid molecules tend to form densely (face-to-face) packed aggregates, which facilitate intermolecular coupling and exciton delocalization, often resulting in the emission quenching. On the other hand, molecules bearing nonplanar structure or rotational side-units can effectively reduce intermolecular interactions by arranging themselves into edge-to-face structures [15,21] or amorphous-like aggregates [25,26], which in either case can promote emission enhancement.

Here, formation of FONs based on novel *p*-phenylenediacetonitrile derivatives by re-precipitation method in aqueous solutions is demonstrated. The exceptionality of the derivatives employed is manifested by nitrile groups-induced steric hindrance effects inhibiting concentration quenching of emission. Consisting of different size and polarity end-groups, phenyl groups in one compound and hexyl-carbazolyl in another, the derivatives were examined and compared in regard to nanoparticle formation morphology, size tunability, spectral signatures, and fluorescence turn-on efficiency.

Figure 1a illustrates the dependence of the shape of **M2** photoluminescence (PL) spectrum on the water content in the solution. The spectrum at 0% of water exhibits well-resolved vibronic structure with dominating zeroth vibronic transition (at 470 nm),

which are typical to those of isolated molecules. The spectral shape remains unchanged by addition of up to 50% of water indicating persistent monomolecular character of

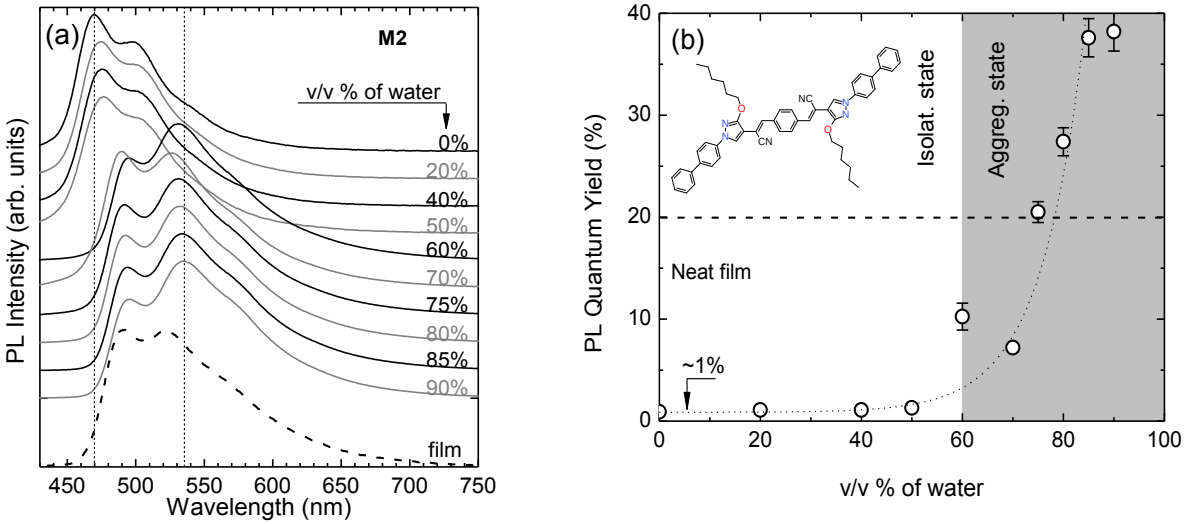

Figure 1. (a) Fluorescence spectra and (b) fluorescence quantum yield of **M2** in THF/water mixtures with different volume percent (v/v %) of water. **M2** concentration in THF/water mixtures was kept constant (1×10^{-5} M). The spectra are vertically shifted for clarity. Dashed lines mark PL data of the neat amorphous film.

fluorescence. A sudden change in the spectral shape occurring just above 50% of water clearly demonstrates formation of the new state with the dominant transition at 535 nm. In accordance with the spectral signature the state persists up to 90% of water fraction. Importantly, the PL band corresponding to this state is not present in the PL spectrum of the neat amorphous film of **M2** (Figure 1a). This indicates that the new state originates from the aggregates with different molecular packing as compared to that in amorphous film. The evolution of the photoluminescence quantum yield (PL QY) of **M2** solutions with increasing water content clearly displays fluorescence turn-on feature at a water fraction of 60% (Figure 1b). The same point also marked the appearance of the new state in the PL spectra due to formation of aggregates. The fluorescence turn-on with increasing non-solvent content has been also reported by others [15,17,20,27], where this feature was attributed to aggregation-induced emission. An increase of water content up to 50% does not alter PL QY of **M2**, which is very low (~1%) in a dilute solution and is totally determined by emission efficiency of non-interacting molecules as evidenced by monomolecular spectrum. The low QY for sterically hindered molecules in dilute solutions is known to be caused by the rotating groups-induced torsional deactivation of

the excited state [28,29]. The increase of the PL QY followed by continuously increasing water content above 50% is promoted by specific aggregation of the **M2** molecules present inside THF droplets. Taking into account complete water miscibility of THF, increasing water content unavoidably reduces size of the THF droplets, and consequently, average intermolecular separation of the **M2** molecules inside the droplets thus forcing them to aggregate. Essentially, the enhancement of PL QY is directly related to the diminishing number of free molecules and growing number/volume of aggregates. Since both free molecules and aggregates are capable of absorbing excitation energy, but only aggregates produce efficient emission, the increasing number of the later is thus responsible for the PL QY enhancement. The maximum PL QY achieved in the **M2** aggregates is 38%, what determines the maximum fluorescence on/off ratio of 38. For comparison, 2-fold lower PL QY is obtained in the amorphous film of **M2**.

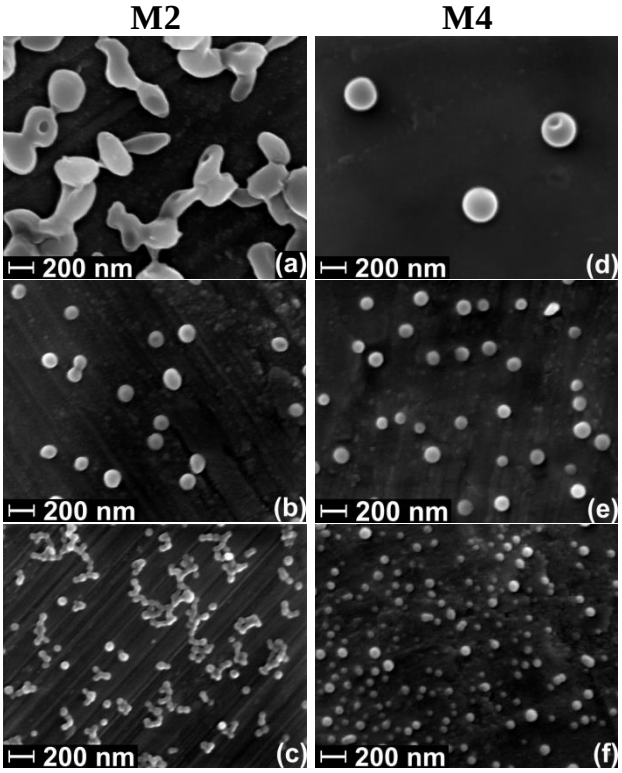

Figure 2. FE-SEM images of **M2** (a), (b), (c) and **M4** (d), (e), (f) nanoparticles formed in THF/water mixtures with 60 (a), (d), 75 (b), (e) and 90 (c), (f) volume percent of water. The solute concentration in the mixture was kept constant (1×10^{-5} M).

The visualization of the phenylenediacetonitrile nanoparticles formed at different THF/water ratios and casted on the aluminum foil was accomplished by using field-emission scanning electron microscopy (Figure 2). FE-SEM images mainly indicate a spherical shape of **M2** and **M4** nanoparticles, which in the case of **M2** for 60% of water become slightly elongated (Figure 2a). The images clearly evidence reduction of the nanoparticle sizes with increasing water content in the THF/water mixture. The mean diameters of the **M2** nanoparticles obtained by averaging over the large ensemble attained the values of 55 nm and 360 nm for 90 and 60 volume percent of water, respectively, whereas for **M4** nanoparticles the mean diameter ranged from 60 nm to 280 nm. FE-SEM results on nanoparticle sizes are in an excellent agreement with those obtained by dynamic light scattering technique.

Taking into account the constant **M2** and **M4** concentration maintained in the THF/water mixtures irrespective of the solvent/nonsolvent ratio, descending nanoparticle size with increasing water content indicates increasing local concentration of the molecules in the THF droplets as well as in the casted nanoparticles. More dense packing of the molecules in the nanoparticles and diminishing number of free molecules with increasing water content is responsible for the steady enhancement of the PL QY and PL decay time.

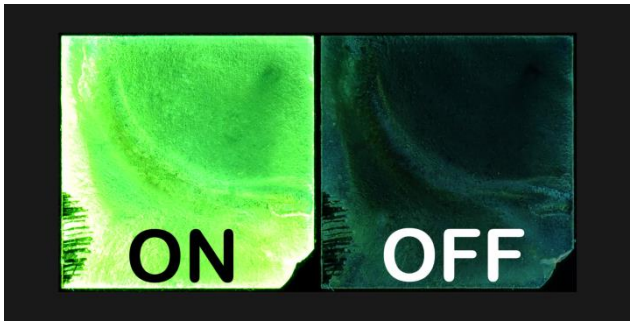

Figure 3. Fluorescence images of **M2** nanoparticle film spin-casted on the glass substrate (a) before and (b) after exposure to THF vapors for 3 min. The photos are taken under UV excitation.

The exposure to different organic vapors of THF, dichloromethane or methanol produced fairly similar result with comparable minute time-scale quenching rate. This demonstration shows the potential of implementation of the phenylenediacetonitrile nanoparticle films for sensing of various organic vapors.

3.1.2. Color changes determined by aggregation of naphthalimide and triphenylamine compounds

In this chapter, we summarise results on emission color changes of donor-acceptor molecules of singly-bonded triphenylamine and naphthalimide upon aggregation and formation of time-temperature sensing layers.

Dipolar triphenylamine and naphthalimide derivatives showed high fluorescence quantum yield (up to 80%) and high of electron and hole mobility values (> 10^{-3} cm^2/Vs) [S8,S10]. Here we focus on solvatochromic behaviour of the compounds. We chose four solvents with different polarity: non-polar toluene (dipole moment – 0.36D), chloroform (1.04D), acetone (2.88D) and polar DMSO (3.96D). Absorbance and fluorescence spectra of **M5**-**M7** molecules in those solvents are presented in figure 4. The shape of absorbance spectra do not change while changing solvent polarity, only the peak of lowest energy band shifts by 15-24 nm by increasing solvent polarity. Also it was observed the increase of extinction coefficient by increasing the number of

naphthalimide arms [S8, S10]. In contrast the PL spectra show pronounced changes with polarity, they are broadened and red-shifted up to 206 nm for **M7** molecule. This is typical when the dipole moment is enhancing in the excited state. CT origin of the excited states was also confirmed by DFT modelling [S8, S10]. The fluorescence quantum yields of dilute solutions strongly depend on the solvent polarity (Figure 4). The largest PL QY of 0.70 was observed for compounds **M6** and **M7** with larger number of 1,8- naphthalimide arms in nonpolar solvent toluene. The compounds show significant decrease of the PL QY down to 0.01 in polar solvent dimethylsulfoxide.

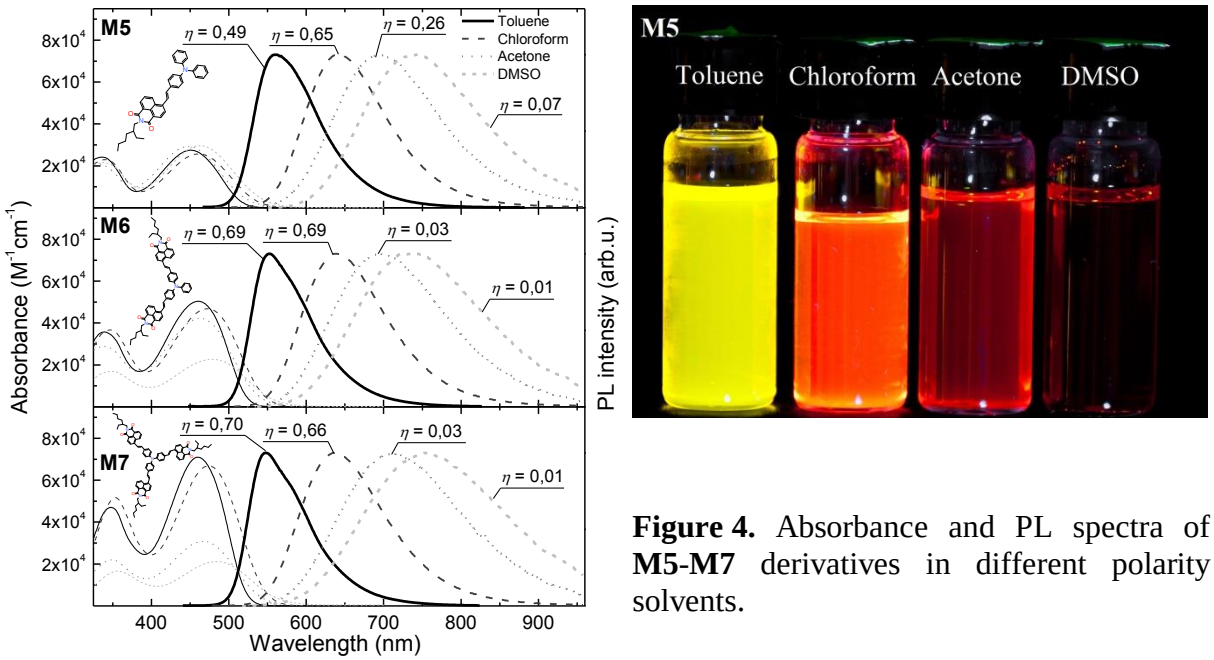

Figure 4. Absorbance and PL spectra of **M5**-**M7** derivatives in different polarity solvents.

The componds show intriguing emission color changes upon aggregation in nonpolar surrounding (polystyrene). Fluorescence pictures of **M5**-**M7** derivatives dispersed in a polystyrene (PS) matrix and neat films excited by UV-LED (365 nm) are presented in table 1. Pictures show that fluorescence spectra gradually changes from green colour in the lowest concentration polymer film to orange in 10wt %. The spectrum of neat film is even more red-shifted. We attribute these color changes to solid state solvation processes.

Table 1 Fluorescence pictures of **M5**-**M7** derivatives embedded with different concentrations in polystyrene matrix and neat films. Excitation: 365 nm UV-LED.

	0.06 wt %	0.25 wt %	1 wt %	4 wt %	10 wt %	Neat film
M5	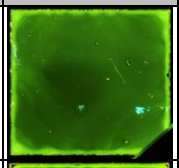	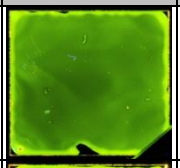	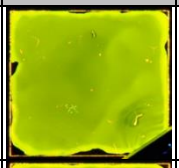	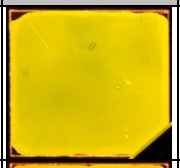	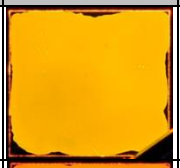	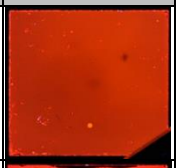
M6	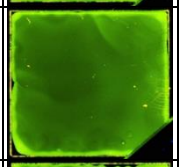	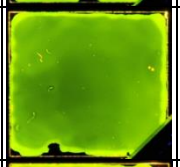	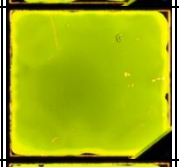	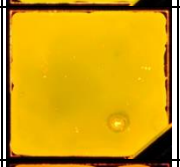	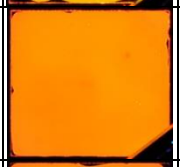	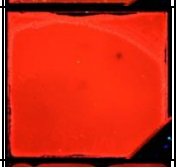
M7	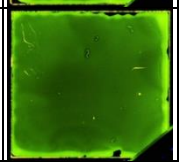	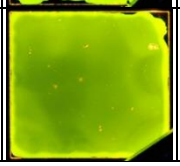	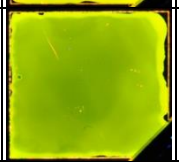			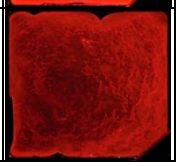

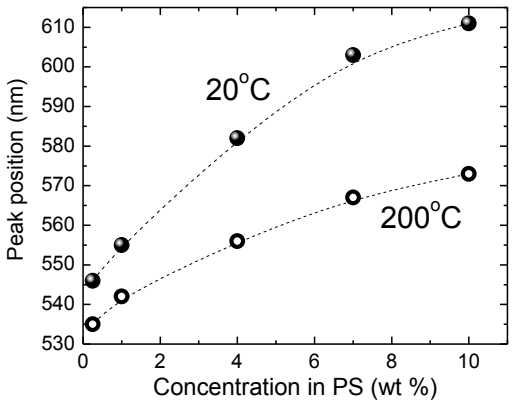

Figure 5. Peak positions of films annealed at different temperature of **M7** embedded with different concentrations in polystyrene matrix.

The biggest spectral change exhibited molecule **M7** was chosen to demonstrate the operation of temperature sensor. **M7** molecule was dispersed in PS matrix, casted on glass substrates and annealed at 100, 150 and 200°C temperature for 24h.

The peak positions of fluorescence spectra of the films are depicted in figure 5. Films annealed at 200°C exhibited blue-shifted spectra with peak positions shifted from 11 to 38 nm. Fluorescence microscopy studies revealed that annealing, as well as increase in dye concentration, leads to enhancement in the nanoaggregate size. However the fluorescence shifts from that typical of aggregate emission to that typical for single molecules, upon annealing. This reverse color change is rather unusual, since typically annealing leads to formation of aggregates and results in significant redshift due to self-trapped exciton formation [30–34]. The red-shift can rationalised by taking into account excitation energy transfer processes from monomer to aggregate species. Thermal treatment results in diffusion of molecules and formation of larger size aggregates, however this also results in enhancement in average distance between single molecules and aggregates. This causes reduced excitation energy transfer and stronger emission of single molecules, thus the blueshift in emission.

3.2. Control of fluorescence concentration quenching

The investigations of solutions have made great input to the major understanding of luminescence processes at molecular level. The assumptions made from the dilute solution data, however, cannot usually be extended to the concentrated solutions. Certainly, many organic chromophores demonstrate very different light-emitting behaviours in dilute and concentrated solutions. For instance, emission is often weakened or quenched at high concentrations, a phenomenon known as concentration quenching [35]. A main reason for the quenching process is associated with the formation of aggregates [35].

In the second part of experimental results, we discuss an opposite case, when fluorescence of the film is quenched by formation of molecular aggregates. The aggregation caused quenching (ACQ) is important for OLED layers fabrication [35, 36]. But it is even more important to organic lasers where the concentration of chromophores could be very high to achieve low stimulated emission thresholds [37,38]. Here we summarize the peculiarities of aggregation induced fluorescence quenching phenomenon in functionalised lasing systems such as perylene diimide, pyrene and DCM laser dye systems.

3.2.2. Bay substituted perylene diimides for laser applications

Perylene tetracarboxylic acid diimide, in short perylenediimide (PDI) derivatives constitute one of the most widely studied molecular system, which, owing to unique combination of physical properties found applications in almost all directions of organic optoelectronics. Based on their high stability, optical and redox properties PDI derivatives are employed in electrophotography (xerographic photoreceptors) [39] and photovoltaics [40]. High electron affinity of rylene diimide dyes and close chromophore packing in the solid state make them one of the best organic electron-transporting materials for thin film transistor applications [41,42]. Recently, air-stable thin film transistors have been demonstrated [43]. Additionally, extended π-conjugation and rigid molecular structure of the PDI core results in a high PL QY, thus making PDI

derivatives attracting as laser dyes [44,45], e.g. famous perylene orange and red dyes, fluorescent light collectors and labels [22,23], fluorescence sensors [46] as well as emitters in organic light emitting diodes (OLED) [47]. It is important to note that PDIs are among the most photostable organic electronic materials reported in literature what is advantageous for optoelectronic applications, in particular for laser applications [48]. If considering PDI derivatives studied in this work, the later application is at our primary focus.

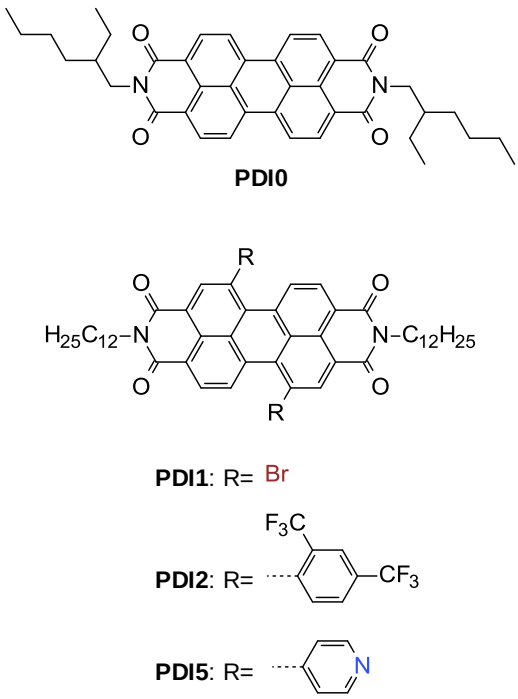

Figure 6. Chemical structures of the PDI derivatives.

Origin of the excited states. Polymer films doped with PDI dye molecules constitute nontrivial objects with optical properties varying from those of molecular-like to crystal-like depending on doping concentration [48–50]. Strong concentration effects might occur as a result of various excitation energy-transfer processes that can be critical for the dye performance in a device [51,52]. To disclose molecular and exitonic spectral properties of the PDI-doped polymer films, absorbance and fluorescence spectra of the PDI0/PS, PDI1/PS, PDI2/PS and PDI5/PS (Fig. 6) films at relatively low 0.06-0.5 wt % and high 8 wt % doping concentrations were investigated (Fig. 7). 0.06 wt % doped PDI0/PS film exhibits spectral behaviour typical of single perylenediimide molecules, which have a narrow 0-0 absorption band at 531 nm accompanied by well-resolved set of vibrational satellites (spaced by 0.17 eV) originating from several internal breathing modes [53]. Corresponding fluorescence bands appear as a mirror-image of the absorption bands and are Stokes-shifted by only 5 nm. This indicates high rigidity of the PDI molecular structure. Similarly, absorption spectra of the PDI1/PS, PDI2/PS and PDI5/PS films doped with the bay-substituted PDIs at low concentration closely resemble those obtained for dilute THF solutions with non-interacting PDI molecules [54]. Small red shift (of about 5 nm) of the PDI/PS spectra in respect to the

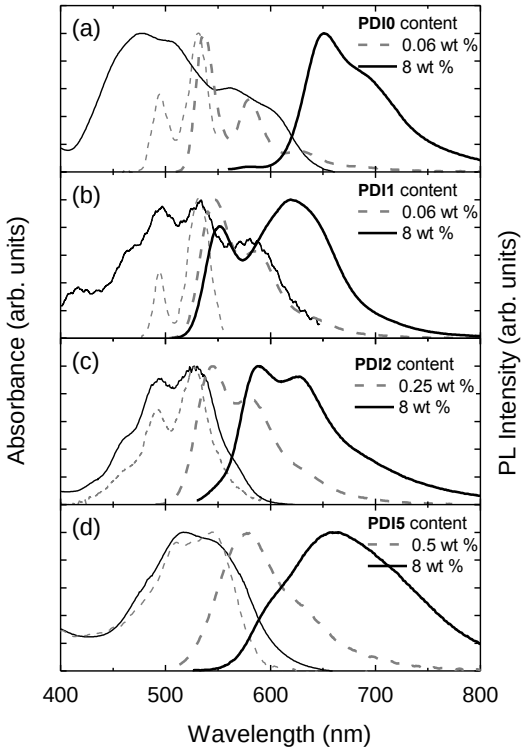

Figure 7. Normalized absorption and fluorescence spectra of a) PDI0/PS films, b) PDI1/PS films, c) PDI2/PS films and d) PDI5/PS films with relatively low 0.06-0.5 wt % (dashed lines) and high 8 wt % (solid lines) PDI-doping concentrations.

PDI solution spectra can be attributed to the different surrounding media of the PDI molecules. Generally, the bay substitution with electron-withdrawing groups causes only slight modifications to the spectral properties of isolated PDI molecules, and consequently, only minor reduction of photoluminescence QY in dilute solutions [54,55]. On the other hand, the bay substitution was reported to have dramatic effect on the spectral properties of the PDIs in a solid state [55]. Indeed, absorbance and fluorescence spectra of highly doped PDI1-5/PS films (solid lines in Fig. 7) demonstrate remarkable modifications of the spectral profiles and maxima positions. The modifications of the excitonic properties are mainly related to different molecular packing caused by the steric hindrance effects. The substitution at the bay position induces two major changes to the planar geometry of the unsubstituted PDI. The first is a twisting of the perylene core by 14-36 degrees depending on a bay-substituent, which generally reduces intermolecular interaction [55], whereas the second geometry modification, i.e. large torsions of the bay substituents in respect to the core, arises from the steric hindrance at the bay regions. Large torsion angles (~70°) between the planes of the perylene core and aromatic bay substituents revealed by DFT calculations inhibit close packing of the PDI2 and PDI5 molecules thus also diminishing intermolecular coupling in a solid state [54]. Meanwhile, owing to the planar geometry of PDI0, the highly doped PDI0/PS film shows very broad absorption spectrum with strongly redshifted lowest energy band at about 625 nm indicating strong excitonic coupling. We attribute this band to J-like (Jelley-Scheibe) aggregates in accordance with the previous reports, where the absorption band located in the range of 621-629 nm for similar PDI derivatives with ethyl-heptyl groups at the imide nitrogen position were attributed to the

J aggregates [56]. Similarly to changes in absorption, fluorescence spectrum of the PDI0/PS film also exhibits pronounced redshift of the emission maximum from 536 nm to 652 nm followed by increase in the chromophore concentration from 0.06 to 8 wt % confirming strong excitonic coupling. Emission spectrum is Stokes-shifted by 27 nm and shows well-expressed vibronic structure typical for excitonic spectrum. It is well-known that the bay substitution of PDIs leads to significant transformation of the excitonic interaction. Incorporation of bromine at 1,7 position of the PDI (compound PDI1) was shown to result in the core twisting by about 24 degrees and reduction of excitonic coupling [54,55]. This is evidenced from the less broadened absorption spectrum and blueshifted lowest-energy absorption band (at about 585 nm) as compared to that due to aggregates of planar PDI0 (see Fig. 7a,b). Bulky 2,4-di(trifluoromethyl)phenyl bay substituents in the PDI2 give rise to both geometrical modifications (PDI core twisting and torsions of the bay-substituents) of the molecule resulting in even stronger suppression of the excitonic interaction. Absorption spectrum of highly doped PDI2/PS film is similar to the molecular spectrum obtained at low chromophore concentration and shows just a slight broadening (Fig. 7c). Correspondingly, the main fluorescence band of highly doped PDI-2/PS film experiences much smaller red shift in respect to the lightly doped PDI-2/PS film as compared to the red shifts of the rest films and a continuous trend of fluorescence band shifting from 625 nm (for PDI0/PS) to 589 nm (for PDI2/PS) can be observed (see solid lines in Fig. 7a-c). Increase of the doping concentration in PDI5/PS film with dopant PDI5 having less polar 4-pyridyl bay substituents also causes a slight broadening of the absorption spectrum with the lowest-energy band at about 560 nm (Fig. 7d), which is attributed to the face-to-face or rotationally displaced face-to-face molecular packing (H-type aggregates) [55]. Fluorescence spectrum of highly doped PDI5/PS film is strongly Stokes-shifted and features broad unstructured band at about 659 nm. This signifies remarkable lattice reorganisation leading to exciton self-trapping, which is commonly observed for face-to-face packing of large aromatic molecules [53,57].

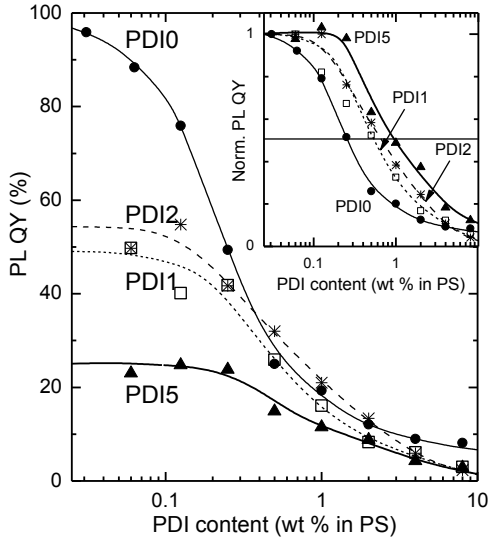

Figure 8. Fluorescence quantum yield of the PDI0/PS films (dots), PDI1/PS films (rectangles), PDI2/PS films (stars) and PDI5/PS films (triangles) as a function of PDI-doping concentration. Lines are guides for the eye. Inset depicts normalized PL QY results of the PDI/PS films vs PDI content.

Fluorescence quenching. Increase in the PDI concentration causes formation of aggregates leading to remarkable fluorescence quenching of the PDI/PS films. Fluorescence QY dependences of the PDI0/PS, PDI1/PS, PDI2/PS and PDI5/PS films on the PDI content for the 0.06 – 8 wt % range are depicted in Fig. 8. At low PDI concentration the reference film PDI0/PS attains QY of 96% that is similar to the value obtained for non-interacting PDI0 molecules in dilute solutions. On the other hand, the films doped with the bay-substituted PDIs (PDI1, PDI2 and PDI5) at low concentration express somewhat lower QY values as compared to those obtained in their solutions. Note that the QY values ranging from 73% to 47% were obtained for the PDI1–PDI5 compounds, respectively, in their dilute solutions [54] and the values from 56% to 26% were estimated for the same compounds in PS films at low doping concentration (Fig. 8). This discrepancy of the QY values in solution and polymer film at low doping level might be attributed to the sensitivity of the bay-substituted PDIs to the polarity of the surrounding media as was reported for bromine bay-substituent [58]. Generally, the reduction of fluorescence QY with incorporation of bay-substitutents in dilute media is known to originate from intramolecular charge-transfer induced by the difference in a polarity of the PDI core and the bay-substituents [54,58].

All the studied PDI derivatives dispersed in polymer matrix at high concentration display very low PL QY (2-8%) (Fig. 8). This decrease of PL QY with increase of the doping concentration suggests formation of aggregate states acting as molecular emission quenchers. Obviously, fluorescence quenching is dependent on the bay-substituents, which govern molecule arrangement in solids via the steric hindrance effects. As it can be seen from the inset of Fig. 8 half of the fluorescence intensity of the unsubstituted planar PDI0 molecules quenches already at 0.24 wt % doping content, whereas fluorescence concentration quenching for the bay-substituted non-planar PDI1,

PDI2 and PDI5 compounds occurs at about 0.5 wt %, 0.6 wt % and 0.9 wt % doping content, respectively. The quenching at the 3-4 times higher doping levels for the polymer films doped with the bay-substituted PDIs is a result of reduced intermolecular interaction due to the less tight packing of the films.

Table 2 Optical properties of the bay-substituted PDI derivatives (PDI1, PD2 and PDI5) and unsubstituted reference PDI compound (PDI0) dispersed in polystyrene film at low and high doping concentration

	PDI content in PDI/PS film 0.06 – 0.5 wt %					PDI content in PDI/PS film 8 wt %			QY_{max}	I_{ASE}^{th} (kW/cm^2)	$t_{0.7}$ (pump pulses)
	λ_{abs} (nm)	λ_{em} (nm)	τ (ns)	τ_{rad} (ns)	τ_{nrad} (ns)	λ_{abs} (nm)	λ_{em} (nm)	τ_{avg} (ns)			
PDI0	495, 531	537, 579	4.9	5.1	123.3	474, 508, 560, 605	650	11.51	0.96	20@0.03 wt %	120×10^3 @40 kW/cm^2
PDI1	494, 532	547, 585	6.6	13.4	12.9	496, 534, 580	552, 619	3.10	0.49	69@0.25 wt %	120×10^3 @200 kW/cm^2
PDI2	493, 526	545, 581	6.1	11.0	13.4	495, 528	589, 628	2.93	0.55	166@0.5 wt %	25×10^3 @300 kW/cm^2
PDI5	510, 545	579	6.7	27.0	9.0	517, 552	662	16.88	0.25	816@0.5 wt %	10×10^3 @1600 kW/cm^2

To reveal the dominating excited state relaxation processes and to support fluorescence QY decrease due to concentration quenching effects, fluorescence transients of the PDI/PS films at various PDI concentrations were measured. At low PDI doping concentrations (<0.5 wt %) the transients could be fairly well approximated by using single-exponential decay model, whereas at high PDI concentration at least two decay components were required to fit the data. Correspondingly, only the average fluorescence lifetime (τ_{avg}) for high PDI content of 8 wt % is given in Table 2. Based on measured fluorescence lifetime and QY results radiative (τ_{rad}) and nonradiative (τ_{nrad}) decay time constants for the PS films with low PDI content were evaluated. Fluorescence lifetimes of the bay substituted PDI1-PDI5 compounds embedded in a PS matrix were found to be slightly longer (see Table 2) as those obtained for the same compounds in THF solution [54]. The radiative relaxation rate was clearly dominant for the isolated molecules of the reference PDI0 compound and this rate determined the character of the excitation relaxation processes in the bay-substituted PDI/PS films at low PDI concentration. At high doping concentration fluorescence lifetime is affected by the nature of exciton-vibronic coupling and exciton transfer processes. Interestingly, an

increase in the PDI-doping concentration resulted in the 2-fold shortening of the fluorescence lifetime for the PDI1/PS and PDI2/PS films, meanwhile in more than 2-fold extension of the lifetime for PDI0/PS and PDI5/PS films. The result can be clarified by the differences in molecular packing of the aggregates indicating the presence of self-trapped excitons in more tightly packed PDI0/PS and PDI5/PS films as it was previously revealed from the excitonic spectral features (see Fig. 7).

Amplified spontaneous emission. Alteration in intermolecular coupling caused by the electron-withdrawing bay-substituents of the PDI compounds severely influences amplified spontaneous emission (ASE) properties of the PDI/PS films. Figure 9 depicts excitation power dynamics of the edge emission of PDI0-PDI5/PS films in the "thin-stripe" geometry [59]. All the PDI/PS films demonstrate broad spontaneous emission spectra structured with vibronic modes, particularly well-resolved for PD0/PS film, at the lowest pump density. Note that the maxima of spontaneous emission spectra measured from the edge are located at the first vibronic replica if compared with the spectral maxima peaked at the zeroth vibronic mode, which are measured in usual backscattering configuration. This is caused by the reabsorption of the short-wavelength tail of the emission band. Increase in the excitation power density of the PDI/PS films at a certain point results in the emission band narrowing indicating an onset of ASE. The ASE band emerges at the spectral position of the first vibronic replica, i.e. at the emission band maximum, which is a typical situation for PDI derivatives since absorption in the spectral region of the zeroth vibronic replica is relatively strong [48]. All of the studied bay-substituted PDI derivatives demonstrate pronounced ASE behavior. Substitution at the bay position enables tuning of the ASE wavelength from 581 nm (for unsubstituted PDI0) to 624 nm (for PDI5). Additionally, some tuning of the ASE peak can be accomplished by changing the dye concentration in the PDI/PS films. For example, variation in the PDI5 content from 0.06 wt % to 4 wt % can shift the ASE peak from 596 nm to 626 nm.

The onset of the ASE can also be verified from the integrated fluorescence intensity dependence on the pump density (see insets of Fig. 9). A sudden change in the intensity dependence from linear to superlinear clearly signifies the onset of the ASE and enables estimation of the excitation intensity threshold values (I_{ASE}^{th}) of the ASE for each PDI/PS

film at various doping concentrations. I_{ASE}^{th} value are important parameter describing the feasibility of the material to be employed in lasing systems as an active media. Evidently, an active material featuring lower I_{ASE}^{th} will require lower operating current density, which is critical for the device formation [37,60].

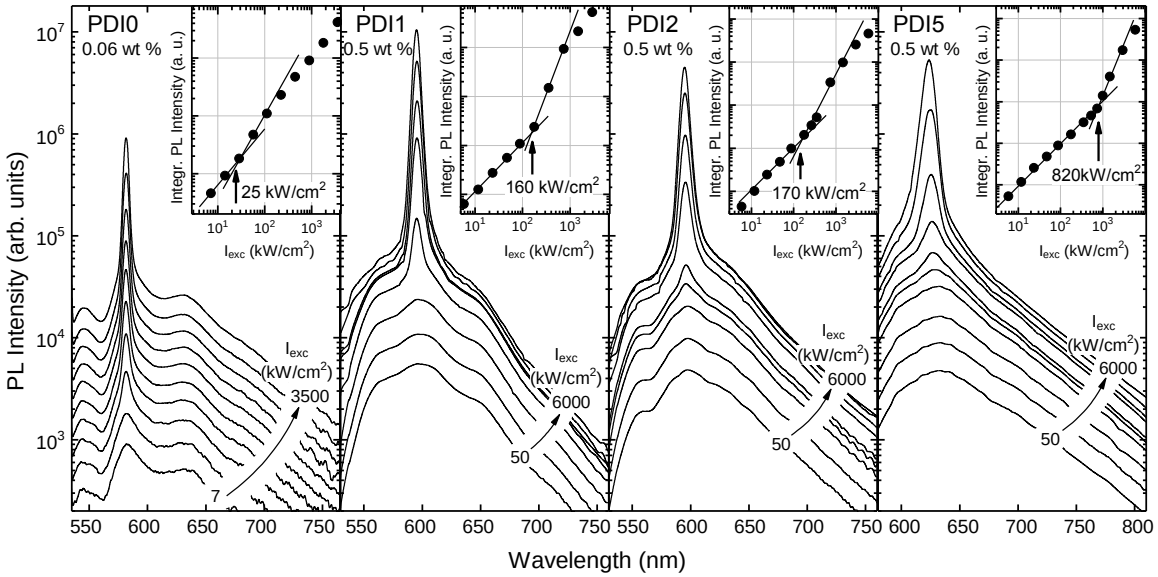

Figure 9. Excitation power dependence of the edge emission spectra of (a) PDI0/PS film, (b) PDI1/PS film, (c) PDI2/PS film and (d) PDI5/PS film doped with 0.125, 0.5, 0.5 and 0.5 wt % of the PDI, respectively. Insets show integrated fluorescence intensities as functions of excitation power densities. The arrows indicate onset of ASE.

Since molecule arrangement plays a major role in obtaining high fluorescence QY and stimulated emission in a solid state, detailed investigations of the ASE performance as a function of the concentration of the active material is of great importance. Moreover, these investigations are indispensable for determination of the optimal concentration for laser operation [48]. Essentially, the ASE performance of the PDI derivatives is rather sensitive to the chromophore concentration. PDI derivatives substituted at the imide nitrogen position was reported to show ASE for concentrations ranging from 0.25 to 5 wt % [48,61], whereas the derivatives additionally substituted at the bay position by tert-butylphenoxy or tert-octylphenoxy groups expressed ASE for concentrations ranging from 1.5 to 3 wt % [62,63].

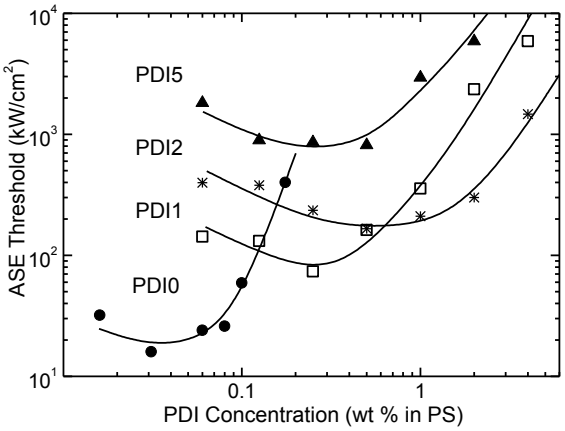

Figure 10. ASE threshold of the PDI0-PDI5/PS films as a function of PDI-doping concentration. Lines are guides for the eye.

PDI concentration dependencies of the I_{ASE}^{th} of the bay-substituted PDI1-PDI5/PS films as well as unsubstituted PDI0/PS film are depicted in Fig. 10. All of the studied PDI/PS films demonstrate nontrivial ASE behaviour with increasing PDI content. At low PDI content I_{ASE}^{th} decreases, while at higher chromophore concentration it increases. Since non-interacting PDI molecules usually exhibit higher fluorescence QY as compared with that of their solids, the onset of ASE initially occurs for the single molecular states. This is also confirmed by the ASE spectral behaviour observed in the PDI/PS films with low PDI content (Fig. 10). Increasing PDI content reduces intermolecular separation and thus diminishes optical losses causing lowering of the I_{ASE}^{th}. However, further increase in the PDI concentration results in the formation of aggregated states with absorption in the emissive region of single PDI molecules. As it was shown in Fig. 8, aggregates of the PDI0-PDI5 derivatives also act as quenchers of molecular emission, and consequently, leads to an increase of the I_{ASE}^{th}. This implies presence of some optimal chromophore concentration range in the PDI0-PDI5/PS films, where favourable conditions for ASE and minimal I_{ASE}^{th} value can be attained. This optimal concentration range for the reference compound PDI0 was determined to be between 0.01 and 0.25 wt %, whereas the minimal I_{ASE}^{th} value was estimated to be as low as 20 kW/cm^2. Note that similar ASE threshold value (15 kW/cm^2) has been reported for the PDI substituted at the imide nitrogen [48]. Although the bay-substituted PDI1–PDI5 derivatives demonstrate remarkably higher I_{ASE}^{th} values, they also feature wider concentration range (0.06 – 4 wt %) favourable for ASE observation, which is shifted by more than one order of magnitude to higher concentrations (see Fig. 10). The minimal I_{ASE}^{th} values of 70 kW/cm^2, 165 kW/cm^2 and 860 kW/cm^2 were obtained for PDI1/PS film doped with 0.25 wt % of bromo-substituted PDI dopant, PDI2/PS film doped with 0.5 wt % of 2,4-di(trifluoromethyl)phenyl-

substituted PDI dopant and PDI5/PS film doped with 0.25 wt % of 4-pyridyl-substituted PDI dopant, respectively. I_{ASE}^{th} values estimated in previous ASE studies were 300 kW/cm^2 for tert-butylphenoxy and 1500 kW/cm^2 for tert-octylphenoxy bay-substituted PDIs dispersed in polystyrene [48,62,63]. It is worth noticing that the obtained ASE threshold values of PDI1 and PDI2 compounds are among the lowest ones observed for the bay-substituted PDIs. Although the minimal I_{ASE}^{th} is significantly lower for the unsubstituted reference compound PDI0, the ASE is rapidly quenched for the chromophore concentration exceeding 0.25 wt %. 2,4-di(trifluoromethyl)phenyl-substituted perylenediimide derivative (PDI2) can be distinguished by the smallest intermolecular coupling due to the bulky bay-substituents resulting in the greatly extended range of doping concentrations (0.06 – 4 wt %) favourable for the ASE observation. The latter result infers realization of spontaneous emission amplification in the PDI2/PS films for the PDI2 concentrations up to 2 wt % at reasonably low I_{ASE}^{th} values of 200-300 kW/cm^2. High doping levels are required for efficient lasers where dye-doped organic matrices are used as gain medium.

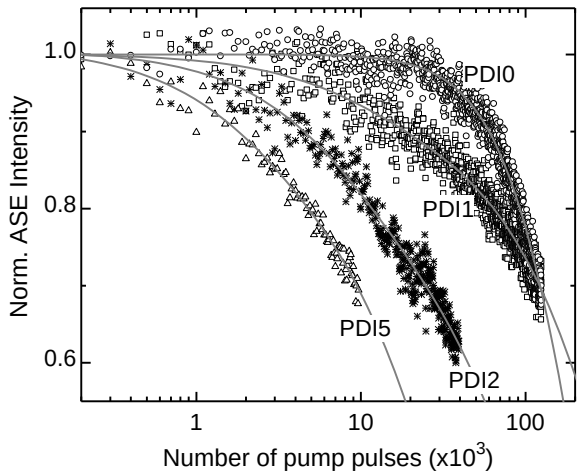

Figure 11. Normalized ASE intensity dependence on the number of pump pulses for PS films doped with PDI0, PDI1, PDI2 and PDI5 at optimal doping concentration of 0.03, 0.25, 0.5 and 0.25 wt%, respectively. The excitation power densities were 40, 200, 300, and 1600 kW/cm^2, respectively.

Photostability. One of the most attractive properties of perylenediimides is their unique photostability [62]. This property is especially important for practical lasing applications, where sufficiently high photon flux must be maintained. The photostability of the PDI0-PDI5/PS films was investigated by recording the integral ASE intensity as a function of the number of pump pulses at constant pump intensity (see Fig. 11). Twice as high pump intensity as the minimal I_{ASE}^{th} for each of the PDI/PS film was used in the photostability measurements. A general tendency of the photodegradation evidenced from a decrease of the total ASE output was observed for all the PDI/PS films. To compare the stability

of lasing PDI/PS films it was defined as the number of pump pulses at which the ASE intensity decayed by 30% of its initial (maximal) value. Very good stability lifetime ($t_{0.7}$) of 120×10^3 pump pulses was obtained for the reference compound PDI0 as well as for the bromo-substituted PDI1 compound. These results are comparable to those obtained for commercially available perylene orange laser dye dispersed in various matrices, like organically modified silica (ORMOSIL) [64] or PMMA [65]. On the other hand, PDI2/PS and PDI5/PS films with the bay-substituted PDI dopants degraded remarkably faster with $t_{0.7}$ of 25×10^3 and 10×10^3, respectively, mainly because of the considerably larger ASE thresholds (see Table 2). Despite of the weaker photostability, our bay-substituted PDI derivatives (PDI1 and PDI2) demonstrate at least an order of magnitude higher photostability as compared to various other organic compounds including other bay-substituted PDIs such as phenoxy-substituted PDIs [62,63].

3.2.4. Fluorene, carbazole and pyrene derivatives for laser applications

One of the most exploited aromatic units constituting the multichromophoric systems are carbazole and fluorene, which, in fact, by proper substitution are capable of delivering multifunctional properties. For instance, carbazoles, known as classic hole-transporters are also utilized as light-emitting materials [66,67]. Meanwhile fluorenes, which are famous for high fluorescence efficiency, easy wavelength-tunability and therefore employed as an active media in OLEDs [68] and organic lasers [69], have been also employed in photovoltaic devices [70].

Previously hardly achievable due to inefficient synthesis routes, carbazole substitution at the 2,7- positions results in a more symmetrical elongated molecule shape, which is beneficial for the preparation of parallel-to-a-substrate oriented molecule layers facilitating light outcoupling from an OLED structure [71,72] and enabling a reduction of amplified spontaneous emission threshold [73].

Integration of the pyrene functional unit into the unified conjugated structure with the fluorene and carbazole chromophores at 2- and 2,7- positions is based on the following arguments. Pyrene moiety has long been known as fluorescent label and probe owing to its tendency of excimer formation, long-lived excited states, high fluorescence

efficiency, and sensitivity of these features to microenvironmental changes [74]. However, it is only recently that pyrene was started to be used as organic semiconductor for advanced applications in materials science and organic electronics. Pyrene-based low-molecular-weight compounds and polymers have been employed as active components in OTFTs [75] and solar cells [74]. Theoretical and experimental findings indicated that suppression of pyrene aggregation by bulky substitutents can result in high solid-state fluorescence quantum efficiencies [76]. Both vacuum deposited [77] and solution-processed [78] layers of fluorene compounds substituted with pyrene at 2-,7-positions were used as efficient blue-emitters in OLEDs. Pyrene-modified oligocarbazoles at 3- and 6- positions were demonstrated to express higher fluorescence quantum efficiencies than the analogous oligomers without pyrene [79]. It is worth noting that there is a lack of reports on the carbazoles substituted with pyrenes at 2,- or 2,7- positions. More recently, pyrene-cored 9,9-dialkylfluorene starbursts were utilized as an optical gain media for low threshold organic semiconductor laser application [80].

Theoretical calculations. As in the case of **FP** and **KP** dyads, **PFP** and **PKP** triads also expressed very similar energy spectra and oscillator strengths for the S_0, S_1 and S_2 states. In principle, the description of the dyads twisted at various angles between pyrene core and fluorine/carbazole in S_0 state is also applicable to triads, since their total energies follow the same trend (Fig. 12). The triads, however, show even wider angular distribution of the corresponding subunits causing $S_0 \rightarrow S_1$ transition to be of comparable strength as that of $S_0 \rightarrow S_2$ at large (or small) dihedral angles. Similarly to the dyads, S_2 state in the triads also expressed energy minima in respect to the twist angle. However, the minima appeared to be slightly deeper and at the larger twist angles (122 deg and 58 deg). The revealed difference between the dyads and triads can be possibly experimentally detected through the intensity variations of the lowest absorption bands corresponding to these transitions.

Electron density in HOMO and LUMO of the **PFP** as well as **PKP** triad is delocalized over the central fluorene(carbazole) and both pyrene subunits in case the subunits are not orthogonal (Fig. 12). Since the triads in the ground state can possess various twist angles (60-120 deg) such the distribution of electron density is highly probable.

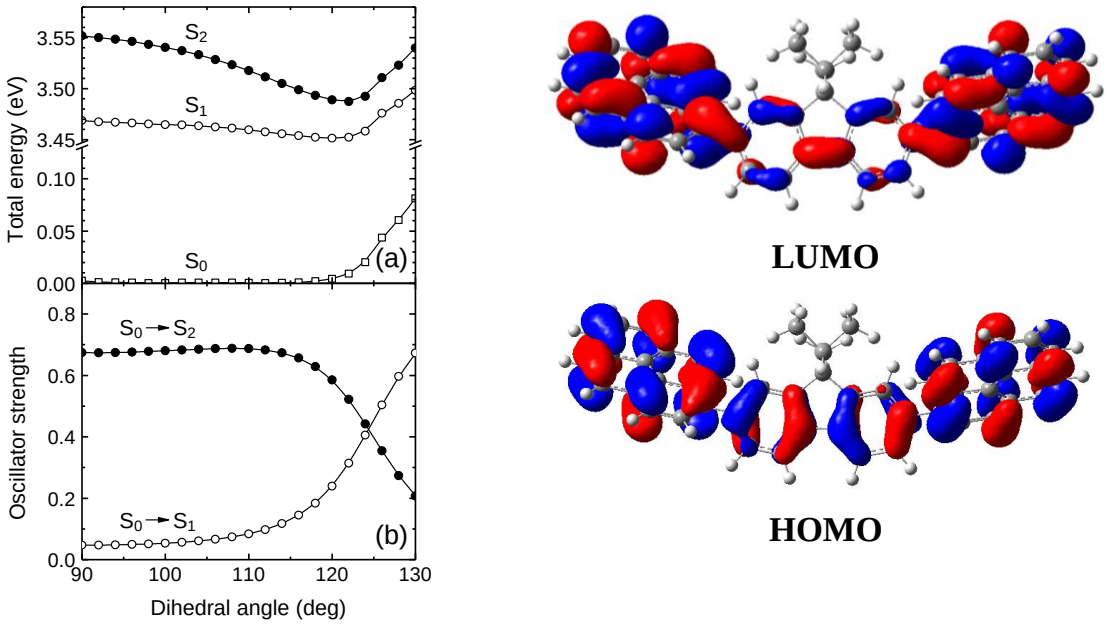

Figure 12. Calculated total energies of the ground state S_0 and the first two excited states S_1, S_2 (a) and oscillator strengths of the singlet transitions $S_0 \rightarrow S_1$, $S_0 \rightarrow S_2$ (b) as a function of dihedral angle for the **PFP** triad. HOMO and LUMO of the **PFP** triad calculated at a dihedral angle of 120 deg using the B3LYP/6-311G (d,p) basis set.

Summarizing the DFT calculation results it is evident that both $S_0 \rightarrow S_1$ and $S_0 \rightarrow S_2$ transitions contribute to the optical spectra of fluorene and carbazole derivatives substituted with pyrene at 2-, 2,7- positions, which is in agreement with other reports on 1-substituted pyrene compounds [81]. A novel result is the low activation energy for the intramolecular twisting of the large singly-bonded chromophores causing the enhanced contribution of the $S_0 \rightarrow S_1$ transition at the large twisting angles (above 120 deg or below 60 deg). Importantly, the triads display conformers with larger twist angles than those of the dyads, and thus, greater impact of the S_1 state, which determines emission properties, the main subject of the present study.

Intramolecular twisting in the excited state. Intramolecular twisting of singly-bonded sterically hindered groups is a frequently observed phenomenon for multifragment compounds [19]. Excited state decay transients of the compounds molecularly dispersed in PS host at concentrations ranging from 1 wt % to 10 wt % were measured and reliably described by double exponential decay model with the dominant decay component having a fractional intensity of over 83%. The estimated dominant lifetimes (τ) for the compounds in PS matrix at low chromophore concentration were found to be 30% longer as to those obtained for the dilute solutions. This provides an

additional prove of the intramolecular twisting in the excited state. The DFT calculations show potential energy minima in the excited states of the dyads and, in particular, of the triads in the vicinity of 120 deg (60 deg) twist angle (Fig. 12a). Possibly, the minima could be more pronounced if the solvation-shell effects were included in the calculations. Since the ground state has the flat potential minimum allowing for a wide distribution of the twist angles, excitation creates differently twisted conformers. In a solution, the excitation migrates to the potential minimum resulting in 120 deg twisted conformers and yielding remarkable shortening of the excited state decay time (down to 1 ns for the triads). Whereas in a rigid PS matrix the intramolecular twisting is restricted implying smaller average twist angle causing emission from the differently twisted conformers and resulting in the observed emission blue shift, nonexponential decay and enhanced average decay time.

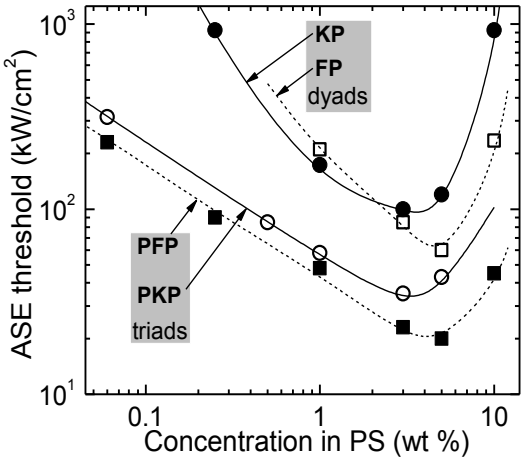

Figure 13. ASE threshold as a function of **FP** (hollow squares), **KP** (filled circles), **PFP** (filled squares) and **PKP** (empty circles) concentration in PS matrix. Lines are guides for the eye.

Extended spectroscopic study of fluorescence concentration quenching and amplified stimulated emission of the perylene derivatives was performed similar to the data presented for PDI componds in the previous section [S4]. Concentration dependencies of I_{ASE}^{th} for **FP**, **KP**, **PFP** and **PKP** molecularly dispersed in PS matrix are illustrated in Figure 13. All the compounds demonstrate rather sensitive ASE performance in respect to the chromophore concentration. At low concentration I_{ASE}^{th} decreases, whereas at higher concentration it increases implying some optimal chromophore concentration, for which I_{ASE}^{th} is the lowest. Since the non-interacting molecules of pyrene-functionalized fluorene and carbazole compounds exhibit higher fluorescence quantum efficiencies as compared to those of their solids and molecularly doped PS with chromophore concentration above 1 wt %, the ASE occurs for the single molecule states. An increase of the chromophore concentration (up to 3 – 5 wt % for our compounds) reduces intermolecular distance and thus diminishes optical losses lowering the I_{ASE}^{th}. However, further increase in the

concentration causes molecule agglomeration to play a decisive role resulting in the aggregation-induced absorption in the spectral region of the amplified emission. This, consequently, enlarges optical losses and rapidly increases I_{ASE}^{th} (Fig. 13).

In accordance with Einstein's B coefficient for stimulated transitions $B \propto (c^3/8\pi h\nu_0^3)k_R$, which is inversely proportional to the I_{ASE}^{th}, the lowest ASE threshold implies the highest radiative decay rate k_R ($k_R = \eta/\tau$). Here c is the velocity of light, ν_0 - the frequency of light and h - Planck's constant. This allows us to rate the compounds according to k_R value, expecting the best ASE performance with the lowest ASE threshold to be demonstrated by the compounds featuring the highest k_R [73]. The calculated k_R for **FP**, **KP**, **PFP** and **PKP** molecularly dispersed in PS matrix at optimal concentration are presented in Table 3. Indeed, as predicted from k_R estimations, **PFP** featuring the highest k_R (3.8×10^8 s^{-1}) demonstrates the lowest I_{ASE}^{th} (20 kW/cm^2), whereas **KP** expressing the lowest k_R (1.1×10^8 s^{-1}) shows the highest I_{ASE}^{th} (100 kW/cm^2). The obtained lowest I_{ASE}^{th} of the pyrene-functionalized fluorene and carbazole derivatives compare well with the ASE threshold values of other classes of small molecule compounds [62] and also with the best ASE threshold values (15-20 kW/cm^2) achieved for 100% emissive perylene derivatives measured in analogous conditions with the compounds dispersed in the inert polymer host [51, S3].

Table 3. ASE properties of the pyrene-functionalized fluorene and carbazole compounds **FP**, **KP**, **PFP** and **PKP** molecularly dispersed in PS matrix at the optimal concentrration.

	c_{opt} [(a)] (wt %)	λ_{ASE} [(b)] (nm)	I_{ASE}^{th} (kW/cm^2)	FWHM [(c)] (nm)	k_R [(d)] $\times10^8$ (s^{-1})
FP	5	424	60	9	1.7
KP	3	424	100	19	1.1
PFP	5	435	20	5	3.8
PKP	3	437	35	13	2.5

(a) Optimal concentration for which I_{ASE}^{th} is the lowest; (b) ASE peak wavelength; (c) Minimal full width at half maximum of the ASE band; (d) Radiative decay rate.

Importantly, the **PFP** and **PKP** triads exhibit lower ASE thresholds than the **FP** and **KP** dyads, which again can be understood via more complex three-dimensional conformations of the triads obstructing closer molecule packing, and thus, diminishing intermolecular coupling and nonradiative decay processes. On the other hand, **FP** and **PFP** bearing bulky dixehyl substituent at fluorene C9 position exhibit lower I_{ASE}^{th} than **KP** and **PKP** containing less bulky ethylhexyl chain at carbazole N9 position, which is

also a consequence of suppressed intermolecular coupling. These ASE results are consistent with the fluorescence spectral and concentration quenching data and suggest that multichromophoric compounds with the larger number of highly-emissive singly-bonded chromophores, owing to their higher emission quantum efficiencies, shorter fluorescence lifetimes and more pronounced steric hindrance effects, are more favorable for application in light-emitting device active layers. Incorporation of optically inactive bulky aliphatic groups into the compounds is advantageous, in particular, for solution-processed thin film layers where they prevent detrimental molecule aggregation.

References

1. T. Kietzke *et al., Nat. Mater.* **2**, 408–412 (2003).
2. H. Gao *et al.*, Nano Lett. **10**, 1440–1444 (2010).
3. T. Piok *et al.*, Adv. Mater. **15**, 800–804 (2003).
4. B. S. Ong, Y. Wu, P. Liu, and S. Gardner, Adv. Mater. **17**, 1141–1144 (2005).
5. C. P. Chan *et al.*, Anal. Chem. **76**, 3638–3645 (2004).
6. H. Y. Kim, T. G. Bjorklund, S.-H. Lim, and C. J. Bardeen, Langmuir **19**, 3941–3946 (2003).
7. J. Jang, J. Ha, and J. Cho, Adv. Mater. **19**, 1772–1775 (2007).
8. S. J. Toal *et al.*, J. Am. Chem. Soc. **127**, 11661–11665 (2005).
9. L. Wang *et al.*, Anal. Bioanal. Chem. **382**, 1300–1303 (2005).
10. H. Liu, J. Xu, Y. Li, and Y. Li, Accounts Chem. Res. **43**, 1496–1508 (2010).
11. W. Herbst and K. Hunger, *Industrial Organic Pigments* (WileyVCH, 2003).
12. T. Asahi, T. Sugiyama, and H. Masuhara, Accounts Chem. Res. **41**, 1790–1798 (2008).
13. B.-K. An, S.-K. Kwon, and S. Y. Park, Angew. Chem. **119**, 2024–2028 (2007).
14. D. Horn and J. Rieger, Angew. Chem. Int. Ed. **40**, 4330–4361 (2001).
15. B. K. An *et al.*, J Am Chem Soc **124**, 14410–14415 (2002).
16. C. Zheng *et al.*, Langmuir **26**, 16730–16736 (2010).
17. H. Tong *et al.*, J. Phys. Chem. C **111**, 2287–2294 (2007).
18. Y. Hong, J. W. Y. Lam, and B. Z. Tang, Chem. Soc. Rev. **40**, 5361–5388 (2011).
19. Z. R. Grabowski, K. Rotkiewicz, and W. Rettig, Chem. Rev. **103**, 3899–4032 (2003).
20. J. Luo *et al.*, Chem. Commun. 1740–1741 (2001).
21. C. J. Bhongale *et al.*, J. Phys. Chem. B **109**, 13472–13482 (2005).
22. S. S. Palayangoda *et al.*, Org. Lett. **10**, 281–284 (2008).
23. K. Itami, Y. Ohashi, and J. Yoshida, J. Org. Chem. **70**, 2778–2792 (2005).
24. M. Han and M. Hara, J. Am. Chem. Soc. **127**, 10951–10955 (2005).
25. D. Xiao *et al.*, J. Am. Chem. Soc. **125**, 6740–6745 (2003).
26. C. Vijayakumar, K. Sugiyasu, and M. Takeuchi, Chem. Sci. **2**, 291 (2011).
27. H. Tong *et al.*, Chem. Commun. 3705 (2006).
28. D. Oelkrug *et al.*, Synth. Met. **83**, 231–237 (1996).
29. J. Ren *et al.*, Dyes Pigments **64**, 179–186 (2005).
30. M. Kinami, B. R. Crenshaw, and C. Weder, Chem. Mater. **18**, 946–955 (2006).
31. B. R. Crenshaw and C. Weder, Adv. Mater. **17**, 1471–1476 (2005).
32. J. Kunzelman *et al.*, Rapid Commun. **27**, 1981–1987 (2006).
33. B. R. Crenshaw *et al.*, Macromol. Chem. Phys. **208**, 572–580 (2007).
34. C. Pietsch *et al.*, Angew. Chem. Int. Ed. **48**, 5653–5656 (2009).
35. J. B. Birks, *Photophysics of Aromatic Molecules* (Wiley-Interscience, 1970).
36. Y. Q. Zhang, G. Y. Zhong, and X. A. Cao, J. Appl. Phys. **108**, 083107 (2010).
37. N. Tessler, Adv. Mater. **11**, 363–370 (1999).
38. E. M. Calzado *et al.*, Org. Electron. **7**, 319–329 (2006).
39. L. Schmidt-Mende, Science **293**, 1119–1122 (2001).
40. J. A. Mikroyannidis *et al.*, J. Phys. Chem. C **113**, 7904–7912 (2009).
41. C. D. Dimitrakopoulos and P. R. L. Malenfant, Adv. Mater. **14**, 99–117 (2002).
42. X. Zhan *et al.*, Adv. Mater. **23**, 268–284 (2011).
43. C. Piliego *et al.*, Adv. Mater. **21**, 1573–1576 (2009).
44. M. Sadrai and G. R. Bird, Opt. Commun. **51**, 62–64 (1984).
45. H. G. Löhmannsröben and H. Langhals, Appl. Phys. B Lasers Opt. **48**, 449–452 (1989).
46. Q. Chen *et al.*, Adv. Funct. Mater. **20**, 3244–3251 (2010).
47. A. Kraft *et al.*, Angew Chem Int End Engl **37**, 402–428 (1998).
48. E. M. Calzado *et al.*, J. Phys. Chem. C **111**, 13595–13605 (2007).
49. C. Karapire, C. Timur, and S. İccli, Dyes Pigments **56**, 135–143 (2003).

50. S. Jursenas *et al.*, Thin Solid Films **516**, 8909–8916 (2008).
51. A. K. Sheridan *et al.*, J. Appl. Phys. **92**, 6367 (2002).
52. S. Lattante *et al.*, J. Appl. Phys. **100**, 023530 (2006).
53. R. Scholz and M. Schreiber, Chem. Phys. **325**, 9–21 (2006).
54. V. Sivamurugan *et al.*, J. Phys. Chem. B **114**, 1782–1789 (2010).
55. Z. Chen *et al.*, Chem. - Eur. J. **13**, 450–465 (2007).
56. S. Ghosh *et al.*, Chem. - Eur. J. **14**, 11343–11357 (2008).
57. M. Matsui *et al.*, Tetrahedron **68**, 9936–9941 (2012).
58. F. Würthner, Pure Appl. Chem. **78**, 2341–2349 (2006).
59. K. L. Shaklee, Appl. Phys. Lett. **18**, 475 (1971).
60. I. D. W. Samuel and G. A. Turnbull, Chem. Rev. **107**, 1272–1295 (2007).
61. E. M. Calzado *et al.*, Appl. Opt. **46**, 3836 (2007).
62. E. M. Calzado, P. G. Boj, and M. A. Díaz-García, Int. J. Mol. Sci. **11**, 2546–2565 (2010).
63. M. A. Díaz-García *et al.*, Synth. Met. **159**, 2293–2295 (2009).
64. Y. Yang, M. Wang, G. Qian, Z. Wang, and X. Fan, Opt. Mater. **24**, 621–628 (2004).
65. N. Tanaka, N. Barashkov, J. Heath, and W. N. Sisk, Appl. Opt. **45**, 3846–3851 (2006).
66. A. Tomkeviciene *et al.*, J. Phys. Chem. C (2011).
67. J. Simokaitiene *et al.*, J. Optoelectron. Adv. Mater. **8**, 876 (2006).
68. B. K. Yap *et al.*, Nat. Mater. **7**, 376–380 (2008).
69. T. Komino *et al.*, Phys. Chem. C **115**, 19890–19896 (2011).
70. C. R. McNeill *et al.*, Adv. Funct. Mater. **18**, 2309–2321 (2008).
71. J.-S. Kim, P. K. H. Ho, N. C. Greenham, and R. H. Friend, J. Appl. Phys. **88**, 1073 (2000).
72. D. Yokoyama, A. Sakaguchi, M. Suzuki, and C. Adachi, Org. Electron. **10**, 127–137 (2009).
73. T. Aimono *et al.*, Appl. Phys. Lett. **86**, 071110 (2005).
74. T. M. Figueira-Duarte and K. Müllen, Chem. Rev. **111**, 7260–7314 (2011).
75. S. Z. Bisri *et al.*, Jpn. J. Appl. Phys. **46**, L596–L598 (2007).
76. Y. H. Park, H. H. Rho, N. G. Park, and Y. S. Kim, Curr. Appl. Phys. **6**, 691–694 (2006).
77. C. Tang *et al.*, J. Mater. Chem. **16**, 4074 (2006).
78. B. Walker *et al.*, Appl. Phys. Lett. **93**, 063302 (2008).
79. Z. Zhao, X. Xu, H. Wang, P. Lu, G. Yu, and Y. Liu, J. Org. Chem. **73**, 594–602 (2008).
80. R. Xia *et al.*, Adv. Funct. Mater. **19**, 2844–2850 (2009).
81. A. G. Crawford *et al.*, J. Am. Chem. Soc. **133**, 13349–13362 (2011).

List of publications related to the thesis:

Papers:

S1. E. Arbaciauskiene, K. Kazlauskas, A. Miasojedovas, S. Jursenas, V. Jankauskas, W. Holzer, V. Getautis, A. Sackus, Pyrazolyl-substituted polyconjugated molecules for optoelectronic applications, *Dyes Pigments*, **85**, 79-85 (2010).

S2. E. Arbaciauskiene, K. Kazlauskas, A. Miasojedovas, S. Jursenas, V. Jankauskas, W. Holzer, V. Getautis, A. Sackus, Multifunctional polyconjugated molecules with carbazolyl and pyrazolyl moieties for optoelectronic applications, *Synth. Met.*, **160**, 490–498 (2010).

S3. A. Miasojedovas, K. Kazlauskas, G. Armonaite, V. Sivamurugan, S. Valiyaveettil, J. Grazulevicius, S. Jursenas, Concentration effects on emission of bay-substituted perylene diimide derivatives in a polymer matrix, *Dyes Pigments*, **92**, 1285-1291 (2012).

S4. S. Krotkus, K. Kazlauskas, A. Miasojedovas, A. Gruodis, A. Tomkeviciene, J.V. Grazulevicius, S. Jursenas, Pyrene-functionalized fluorene and carbazole derivatives for blue light emitters, *J. Phys. Chem. C* **116** (13), 7561–7572 (2012).

S5. A. Vembris, I. Muzikante, V. Gulbinas, R. Karpicz, A. Miasojedovas, S. Jursenas, Fluorescence and amplified spontaneous emission properties of glass forming styryl-4H-pyran-4-ylidene fragment containing derivatives, *J. Lumin*, **132**, 2421-2426 (2012).

S6. A. Vembris, E. Zarins, J. Jubels, V. Kokars, I. Muzikante, A. Miasojedovas, S. Jursenas, Synthesis and optical properties of red luminescent symmetric styryl-4H-pyran-4-ylidene fragment containing derivatives, *Opt. Mater.*, **34**, 1501–1506 (2012).

S7. K. Kazlauskas, A. Miasojedovas, D. Dobrovolskas, E. Arbaciauskiene, V. Getautis, A. Sackus, and S. Jursenas, Self-assembled nanoparticles of *p*–phenylenediacetonitrile derivatives with fluorescence turn-on, *J. Nanopart. Res.*, **14**, 877:1–13 (2012).

S8. D. Gudeika, A. Michaleviciute, J.V. Grazulevicius, R. Lygaitis, S. Grigalevicius, V. Jankauskas, A. Miasojedovas, S. Jursenas, G. Sini, Structure Properties Relationship of Donor–Acceptor Derivatives of Triphenylamine and 1,8-Naphthalimide, *J. Phys. Chem. C*, **116** (28) 14811–14819 (2012).

S9. R.R. Reghu J.V. Grazulevicius, J. Simokaitiene, A. Miasojedovas, K. Kazlauskas, S. Jursenas, P. Data, K. Karon, M. Lapkowski, V. Gaidelis, V. Jankauskas, Glass-Forming Carbazolyl and Phenothiazinyl Tetra Substituted Pyrene Derivatives: Photophysical, Electrochemical, and Photoelectrical Properties, *J. Phys. Chem. C*, **116** (30) 15878–15887 (2012).

S10. D. Gudeika, J.V. Grazulevicius, V. Jankauskas, A. Miasojedovas, S. Jursenas, G. Sini, New derivatives of triphenylamine and naphthalimide as ambipolar organic semiconductors. Experimental and theoretical approach, (submitted to *J. Phys. Chem. C* journal).

S11. D. Gudeika, R.R. Reghu, J. Simokaitiene, J.V. Grazulevicius, A. Miasojedovas, S. Jursenas, V. Jankauskas, Electron-transporting fluorenyl substituted naphthalimides: thermal, photophysical and electrochemical properties, (accepted to *Dyes Pigments* journal).

Presentations at the conferences (underlined A.M. – presented personally):

K1. A. Miasojedovas, R. Sičiūtė, K. Kazlauskas, S. Juršėnas, V. Getautis, „Fluorescent nanoparticles formation from phenylenediacetonitrile compounds“, 10-th International Conference-School, “Advanced materials and technologies“ (August 27-31, 2008, Palanga).

K2. A. Miasojedovas, K. Kazlauskas, S. Juršėnas, D. Dobrovolskas, G. Tamulaitis, E. Arbačiauskienė, V. Getautis, W. Holzer, A. Šačkus, „Fluorescuojančių nanodalelių iš

pirazolo ir nitrilo grupėmis pakeistų dietenų formavimasis“, 38-oji Lietuvos Nacionalinė Fizikos Konferencija (June 8-10, 2009, Vilnius).

K3. K. Kazlauskas, A. Miasojedovas, S. Juršėnas, D. Dobrovolskas, G. Tamulaitis, E. Arbačiauskienė, V. Getautis, W. Holzer, A. Šačkus, „Fluorescent organic nanoparticles based on pyrazole- and cyano-substituted diethenes“, V International Krutyn Summer School, „Organic Electronics: from Lab to Home“ (June 2-8, 2009, Krutyn, Masurian Lake District, Poland).

K4. A. Miasojedovas, K. Kazlauskas, S. Juršėnas, D. Dobrovolskas, G. Tamulaitis, E. Arbačiauskienė, V. Getautis, A. Šačkus, „Formation of fluorescent nanoaggregates based on cyano-substituted diethenes“, 11-th International Conference-School, “Advanced materials and technologies” (August 27-31, 2009, Palanga).

K5. A. Miasojedovas, K. Kazlauskas, D. Dobrovolskas, G. Tamulaitis, S. Juršėnas, E. Arbačiauskienė, V. Getautis, A. Šačkus, „Organinių nanodalelių formavimas, fluorescencija ir mikroskopija“ Pirmoji jaunųjų mokslininkų konferencija, Fizinių ir technologijos mokslų tarpdalykiniai tyrimai (February 8, 2011, Vilnius). (žodinis)

K6. L. Skardžiūtė, K. Kazlauskas, A. Miasojedovas, E. Arbačiauskienė, V. Getautis, A. Šackus, D. Dobrovolskas, G. Tamulaitis, S. Juršėnas, “Aggregation-Induced Emission in p-Phenylenediacetonitrile Nanoparticles”, 4th International Symposium on Flexible Organic Electronics ISFOE-11 (July 10-13, 2011, Thessaloniki, Greece).

K7. A. Vembris, I. Muzikante, R. Karpicz, V. Gulbinas, S. Juršėnas, A. Miasojedovas, „Lumenescenc properties of styryl-4h-pyran-4-ylidene fragment containing derivatives”, 12th International Conference Electronic and Related Properties of Organic Systems ERPOS-12 (July 11-13, 2011, Vilnius).

K8. A. Miasojedovas, K. Kazlauskas, E. Arbačiauskienė, V. Getautis, A. Šackus, D. Dobrovolskas, G. Tamulaitis, S. Juršėnas, “*p*-phenylenediacetonitrile nanoparticles with fluorescence turn-on”, 12th International Conference Electronic and Related Properties of Organic Systems ERPOS-12 (July 11-13, 2011, Vilnius).

K9. S. Juršėnas, K. Kazlauskas, A. Miasojedovas, G. Armonaitė, A. Gruodis, J. V. Gražulevičius, V. Sivamurugan, S. Valiyaveettil, “Concentration Quenching of Amplifield Spontaneous Emission in Bay-substituted Perylenediimides”, 12th International Conference Electronic and Related Properties of Organic Systems ERPOS-12 (July 11-13, 2011, Vilnius).

K10. A. Miasojedovas, K. Kazlauskas, G. Armonaite, R. Karpic, V. Gulbinas, J.V. Grazulevicius, V. Sivamurugan, S. Valiyaveettil, S. Jursenas, “Amplified spontaneous emission in bay-substituted perylenediimides”, 13-th International Conference-School, “Advanced materials and technologies” (August 27-31, 2011, Palanga).

K11. S. Krotkus, A. Miasojedovas, K. Kazlauskas, A. Tomkevičienė, J.V. Gražulevičius, S. Juršėnas, “Novel blue-emitting pyrene-substituted fluorene and carbazole derivatives for lasing application”, 13-th International Conference-School, “Advanced materials and technologies” (August 27-31, 2011, Palanga).

K12. K. Kazlauskas, A. Miasojedovas, D. Dobrovolskas, E. Arbaciauskiene, V. Getautis, A. Sackus, S. Jursenas, “Aggregation-induced fluorescence turn-on in self-assembled 1,4-divinylbenzene nanoparticles”, 13-th International Conference-School, “Advanced materials and technologies” (August 27-31, 2011, Palanga).

K13. A. Miasojedovas, K. Kazlauskas, D. Dobrovolskas, E. Arbaciauskiene, V. Getautis, A. Sackus, S. Jursenas, “Nanoparticles of cyano moieties containing 1,4-divinylbenzene derivatives with fluorescence turn-on”, Baltic polymer symposium BPS 2011 (September 21-24, 2011, Parnu, Estonia).

K14. D. Gudeika, J.V. Gražulevičius, R. Lygaitis, A. Miasojedovas, S. Juršėnas, “Synthesis and properties of glass-forming 1,8-napthtalimide derivatives”, Baltic polymer symposium BPS 2011 (September 21-24, 2011, Parnu, Estonia).

K15. S. Krotkus, A. Miasojedovas, K. Kazlauskas, A. Tomkevičienė, J.V. Gražulevičius, S. Juršėnas, "Blue-emitting pyrene-substituted fluorene and carbazole derivatives for lasing application", 39-oji Lietuvos Nacionalinė Fizikos Konferencija (October 6-8, 2011, Vilnius).

K16. A. Miasojedovas, K. Kazlauskas, G. Armonaite, R. Karpic, V. Gulbinas, J.V. Grazulevicius, V. Sivamurugan, S. Valiyaveettil, S. Jursenas, "Amplified spontaneous emission in perylenediimides substituted at bay positions", 39-oji Lietuvos Nacionalinė Fizikos Konferencija (October 6-8, 2011, Vilnius).

K17. K. Kazlauskas, A. Miasojedovas, D. Dobrovolskas, E. Arbačiauskienė, V. Getautis, A. Šačkus, S. Juršėnas, "Aggregation-induced fluorescence in *p*-phenylenediacetonitrile nanoparticles", 39-oji Lietuvos Nacionalinė Fizikos Konferencija (October 6-8, 2011, Vilnius).

K18. K. Kazlauskas, A. Miasojedovas, D. Dobrovolskas, E. Arbačiauskienė, V. Getautis, A. Šačkus, S. Juršėnas, "Self-assembled fluorescent nanoparticles based on *p*-phenylenediacetonitrile compounds", International Symposium on Functional π-Electron Systems Fπ10 (October 13-17, 2011, Beijing, China).

K19. S. Jursenas, K. Kazlauskas, A. Miasojedovas, G. Armonaite, R. Karpic, V. Gulbinas, J.V. Grazulevicius, V. Sivamurugan, S. Valiyaveettil, "Amplified spontaneous emission in bay-substituted perylenediimides", International Symposium on Functional π-Electron Systems Fπ10 (October 13-17, 2011, Beijing, China).

K20. G. Armonaitė, K. Kazlauskas, A. Miasojedovas, S. Valiyaveettil, J.V. Gražulevičius, S. Juršėnas „Stimulated emission and concentration quenching of perylene diimide derivatives", Open Readings 2012 (Kovo 28-31, 2012, Vilnius).

K21. S. Krotkus, K. Kazlauskas, A. Miasojedovas, A. Gruodis, S. Juršėnas, „Pyrenyl-functionalized fluorene and carbazole derivatives as blue light emitters", Open Readings 2012 (March 28-31, 2012, Vilnius).

K22. G. Kreiza, K. Kazlauskas, A. Miasojedovas, E. Arbačiauskienė, V. Getautis, A. Šačkus, S. Juršėnas, „Formation of fluorescent organic nanoparticles based on 1,4-divinylbenzene derivatives", Open Readings 2012 (March 28-31, 2012, Vilnius).

K23. S.Jursenas, S.Krotkus, K. Kazlauskas, A. Miasojedovas, A.Gruodis, A. Tomkeviciene, J. V. Grazulevicius, „In search for efficient blue-light emitters", Int. Conf. Functional Materials & Nanotechnologies (April 17-20, 2012 Riga, Latvia).

K24. S.Jursenas, S.Krotkus, K. Kazlauskas, A. Miasojedovas, A.Gruodis, A. Tomkeviciene, J. V. Grazulevicius, „Pyrenyl-functionalized fluorene and carbazole derivatives as blue light emitters", IX International Krutyn Summer School, (June 12-18, 2012, Krutyn, Masurian Lake District, Poland).

K25. S.Jursenas, S.Krotkus, K. Kazlauskas, A. Miasojedovas, A.Gruodis, A. Tomkeviciene, J. V. Grazulevicius, „Pyrenyl-functionalized fluorene and carbazole derivatives as blue light emitters", V International conference on molecular materials MOLMAT 2012 (July 3-6, 2012, Barcelona, Spain).

K26. D. Gudeika, J.V. Gražulevičius, A. Miasojedovas, S. Jursenas, V. Jankauskas, „Donor-acceptor derivatives with triphenylamino core and 1,8-naphthalimide arms", XXI International Materials Research Congress 2012, (August 12-17, 2012, Cancun, Mexico).

K27. A. Miasojedovas, D. Gudeika, A. Micheleviciute, R. Lygaitis, S. Grigalevicius, J.V. Gražulevičius, S. Juršėnas, "Fluorescence properties and sensing ability of naphthalimide derivatives", 6th International Meeting on Molecular Electronics ElecMol'12 (December 3-7, 2012, Grenoble, France).

K28. K. Kazlauskas, G. Kreiza, A. Miasojedovas, E. Arbačiauskienė, A. Šačkus, S. Juršėnas, „Tuning of the optical and morphological properties of p-divinylbenzene-based fluorescent nanoparticles", The 10th International Conference on Optical Probes of

Conjugated Polymers and Organic Nanostructures (July 14-19, 2013, Durham, United Kingdom). (oral)

K29. A. Miasojedovas, V. Jankauskas, G. Sini, D. Gudeika, A. Michaleviciute, R. Lygaitis, S. Grigalevicius, J.V. Grazulevicius, S. Jursenas, „Triphenylamine and naphthalimide derivatives as multicolor emitters“, The 10th International Conference on Optical Probes of Conjugated Polymers and Organic Nanostructures (July 14-19, 2013, Durham, United Kingdom).

K30. A. Miasojedovas, V. Jankauskas, G. Sini, D. Gudeika, A. Michaleviciute, R. Lygaitis, S. Grigalevicius, J.V. Grazulevicius, S. Jursenas, "Triphenylamine and naphthalimide derivatives for optoelectronic applications", SPIE Optics + Photonics (August 25-29, 2013, San Diego, United States).

Author's contribution.

The author of this thesis made all the experiments of optical characterisation of all materials, analysed data of measurements. The author prepared manuscripts for the most of papers, also participated in preparation of conference presentations. Part of results were obtained in collaboration with other laboratories: synthesis of materials were performed in prof. J. V. Gražulevičius, prof. V. Getautis, prof. S. Valiayveettil and prof. V. Kokars groups; the ASE measurements of DCM derivatives were performed in prof. V. Gulbinas laboratory; SEM pictures of FON's were performed by dr. A. Kadys; confocal microscopy pictures were obtained by PhD student D. Dobrovolskas; theoretical calculations were performed by dr. A. Gruodis and dr. G. Sini.

Information about the author:

First name	Arūnas
Last name	Miasojedovas
Birth date and place	1984-09-19, Vilnius, Lithuania
E-mail address:	arunas.miasojedovas@ff.vu.lt

Education

2003 – 2007 Bachelor degree Thesis title	Vilnius University, Faculty of Physics (Lithuania) Applied physics study programme "Series Resistance in High Power Light-Emitting Diodes"
2007 – 2009 Master degree Thesis title	Vilnius University, Faculty of Physics (Lithuania) Materials science and semiconductors physics study programme "Formation of Fluorescent Nanoparticles Based on Cyano-substituted Diethenes"
June 2012- September 2012	Visiting student in Durham University, Organic Electroactive Materials group (UK). Project: "Triplet harvesting in OLEDs via triplet fusion - fabrication of deep blue fluorescent OLEDs from anthracene derivatives".
2009 – 2013 Doctoral studies Thesis title	Vilnius University, Faculty of Physics (Lithuania) Graduate studies in physics "Tuning of fluorescence properties of organic optoelectronic materials by forming molecular aggregates"

Scientific work experience

2013 - present	Durham University, Organic Electroactive Materials group (UK) Post-Doctoral Research Assistant Optical spectroscopy, OLED device fabrication.
2006 – 2013	Vilnius University, Institute of Applied Research (Lithuania) Junior Researcher Optical spectroscopy of organic materials for organic light emitting diode applications.
2007 – 2009	Semiconductor Physics Institute, Laboratory of Electrical Standarts (Lithuania), Metrologist. (part-time) Responsible for the support of electrical metrological standard.